This is the Accepted Manuscript version of an article published by Elsevier in the journal *Cities* in 2026, which is available at: https://doi.org/10.1016/j.cities.2025.106516
Cite as: Chen Y, Yang X, Li X, Yang L, Cheng S, Tang G, Biljecki F (2026): Vertical 15-minute city: Modeling urban density and functional mix with multi-source geospatial data. *Cities*, 169: 106516.

Vertical 15-Minute City: Modeling urban density and functional mix with multi-source geospatial data

Yang Chen[a,b,c,d], Xin Yang[a,c,d,e,*], Xin Li[a], Ling Yang[a], Sifan Cheng[b,f], Guoan Tang[a,c,d,e], Filip Biljecki[b,g]

[a]*School of Geography, Nanjing Normal University, No.1 Wenyuan Road Qixia District, Nanjing, 210023, China*
[b]*Department of Architecture, National University of Singapore, 4 Architecture Drive, Singapore, 117356, Singapore*
[c]*State Key Laboratory of Climate System Prediction and Risk Management, Nanjing Normal University, No.1 Wenyuan Road Qixia District, Nanjing, 210023, China*
[d]*Key Laboratory of Virtual Geographic Environment (Nanjing Normal University), Ministry of Education, No.1 Wenyuan Road Qixia District, Nanjing, 210023, China*
[e] *Jiangsu Centre for Collaborative Innovation in Geographical Information Resource Development and Application, No.1 Wenyuan Road Qixia District, Nanjing, 210023, China*
[f]*School of Architecture,Chinese University of Hong Kong, Room G05, Lee Shau Kee Architecture Building, The Chinese University of Hong Kong, Shatin, New Territories, Hong Kong, China*
[g]*Department of Real Estate, National University of Singapore, 15 Kent Ridge Drive, Singapore, 119245, Singapore*

Abstract

The 15-minute city concept emphasizes accessible urban living by ensuring essential services are reachable within walking or biking distance. However, most evaluations rely on two-dimensional (2D) analyses, neglecting the vertical complexity of high-density cities. This study introduces a 3D framework for assessing 15-minute accessibility in Nanjing, China. Using natural language processing and rule-based methods, we construct a 3D functional composition dataset from multi-source data. We then develop floor-level proximity indices that account for both horizontal travel time and vertical circulation (e.g., stairs, elevators). Analyzing over 90 million simulated trips, we find that accessibility generally declines with building height, though

*Corresponding author
Email address: xxinyang@njnu.edu.cn (Xin Yang)

access to offices and commercial facilities improves at 20th or higher floors. Spatial inequalities emerge not only between central and peripheral zones but also across building levels and regional GDP levels, with a U-shaped disparity tied to distance from downtown. Notably, 11%–17% of trips considered accessible in 2D analyses exceed the 15-minute threshold when vertical travel is included. Our findings highlight the need to incorporate vertical space in 15-minute city evaluations and offer a scalable method to support inclusive, fair, and livable 3D urban planning with the background of 15-minute city.

Keywords: 15-minute city, 3D urban function, 3D urban analysis, high-density city, mixed-use

1. Introduction

As urban populations continue to grow, cities increasingly adopt mixed-use and vertical development strategies to accommodate diverse needs within limited land resources [1, 2, 3]. Vertical dimension introduces both opportunities and challenges for our daily life. Vertically mixed-use floors enable residents to live, work, and access essential services within the nearby buildings [4], seamlessly integrating multiple functions into the vertical urban environment [5, 6]. For instance, high-rise buildings may contain grocery stores and restaurants on lower floors, with residential units above, allowing residents to meet daily needs such as shopping or dining without leaving the building. This spatial arrangement enhances mobility efficiency by reducing the need for long-distance travel and concentrating diverse functions within walkable vertical spaces, thereby supporting sustainable, human-centered urban environments [7, 8, 9, 10]. Especially in high-density Asian megacities such as Hong Kong and Tokyo, where land scarcity and large-scale transit hubs prevail, vertical circulation between floors and buildings has become a critical aspect of daily mobility. These vertically integrated, mixed-use spaces embody the core principles of the "15-minute city" concept [11]. In contrast, high-rise developments may undermine functionality and lead to spatial mismatches in low-density contexts [12], and also impose additional vertical travel costs on residents, such as elevator waiting times or barriers for mobility-impaired groups.

The 15-minute city framework proposes that all essential services, such as education, healthcare, recreation, and retail, should be accessible within 15-minute walking or cycling from one's residence [13, 14]. This concept has been an aspiration in numerous global megacities [15, 16] and builds upon earlier urban planning concepts such as the compact city [17, 18], the walkable city [19, 20], chrono urbanism [21] and walkable neighborhoods [22, 23]. It emphasizes spatial proximity as a strategy to reduce travel distances, limit reliance on motorized transport to create sustainable cities, and promote spatial equity to have fair and inclusive urban space [24, 25].

Proximity is central to the evaluation of 15-minute city [26]. Generally, researchers generate 15-minute reachable areas from selected origins and assess the intersection with nearby facilities to quantify local accessibility [27]. These proximity-based spatial measures are widely used to support neighborhood-scale planning and service optimization. However, most existing studies are simple - they only conduct proximity assessments in 2D space, using horizontal road-network distance as a proxy [28]. In the compact and vertical urban environments, this approach overlooks critical components of real-world mobility, such as the time spent navigating stairs, waiting for elevators, and moving between floors [29, 30]. Further, these studies operate at a coarse spatial resolution, potentially resulting in biased assessments. As a result, there is a need to revisit and extend the traditional evaluation framework of the 15-minute city to account for vertical accessibility in vertical urban environment.

Incorporating the vertical dimension in the 15-minute city concept is important for the inclusive, livable, and equitable city, especially for people with disabilities. Therefore, to advance the evaluation of the 15-minute city in high-density, 3D urban contexts, this study identifies and seeks to address the following key research questions:

- RQ1: How can the 3D locations and functional composition of facilities in a building be determined using emerging urban data sources?
- RQ2: How can proximity-related indices be improved to quantify 15-minute accessibility in vertical urban environment, incorporating both network-based and vertical travel distances?

- RQ3: What are the spatial inequalities of 3D 15-minute accessibility in high-density cities, and how are these patterns associated with physical urban form?

In response to the limitations of existing approaches, this study aims to extend traditional 2D 15-minute city evaluations into vertical urban environment by proposing improved 3D proximity indices at the floor level for assessing spatial equity. Specifically, we propose a framework that leverages multi-source urban data to advance the evaluation of 15-minute city vertical accessibility in vertical urban environment. By integrating POIs, AOIs, and land use parcels data, we seek to infer the functional composition of individual building floors. This concept, referred to as "3D functional composition" in this study, denotes the number and floor area of different functions present on each floor within a building, which enables the construction of 3D 15-minute proximity indices that incorporate both horizontal network travel time and vertical movement within buildings. We further examine the spatial distribution of accessibility to identify potential inequalities across building levels and urban zones. Given the complexity of these disparities, we also explore their associations with urban form. Through this integrative framework, the study aims to enhance understanding of 15-minute proximity in high-density, vertical urban environment and to provide methodological insights for future evaluations of vertical equity in urban planning.

2. Related works

2.1. Representative practices of 15-minute city

A growing body of research has emerged to evaluate the progress and implementation of 15-minute city strategies across various global contexts [31, 32], particularly in support of sustainable development goals and the creation of more livable urban environments. This topic has gained significant momentum in European cities, where 15-minute planning principles are increasingly embedded into urban agendas [33]. In large European cities and countries, recent studies have assessed the inequalities in 15-minute accessibility, revealing considerable differences when analyzed from place-based versus individual-based perspectives [34]. One of the most well-known references is Barcelona's "superblock" model, which has been widely studied. Most residents in this dense and compact city live within walking distance of key services, demonstrating the practical viability of the 15-minute framework in high-density settings [35, 36]. In contrast, in more car-centric contexts such as the United States, recent assessments across major cities have incorporated multiple travel modes—such as driving, walking, and cycling—to reflect the diversity of urban mobility patterns [37]. These evaluations reveal substantial variation in the adoption and effectiveness of the 15-minute city concept across different metropolitan areas.

2.2. Definitions and choices of trip origins

The assessment of the 15-minute city is fundamentally based on three key components: trip origins, destinations (amenities), and travel duration [38, 39]. The definition of trip origins in the context of 15-minute city assessments varies across previous studies. Some studies have used a range of origins, including aggregated spatial units, statistical grids, and individual home addresses, to evaluate compliance with the 15-minute city concept.

Most existing studies focus on global or regional scales, where aggregated units such as city blocks [40, 41], census tracts [42, 43], and grid cells [44, 45] are commonly used as trip origins. These approaches commonly rely on low-resolution population or socioeconomic datasets to explore the relationship between accessibility and the urban environment. Consequently, the geometric centroid of these spatial units is used as a proxy for the origin location. While computationally efficient, this method is often simplistic, as it neglects the internal heterogeneity and residential density distribution within the units. This simplification can introduce bias into the accessibility results, particularly in low-density areas. To improve spatial resolution, some studies have adopted finer-scale origin definitions, such as individual home locations [46, 47] or building footprints [48, 49]. These approaches allow for a more detailed and accurate representation of accessibility patterns, enabling refined evaluations of the 15-minute city at the building or household level. However, even these granular methods often overlook vertical heterogeneity. In particular, the vertical distribution of residential units within high-rise buildings, an increasingly dominant urban form in high-density cities, is rarely considered. This oversight overlooks important variations in travel effort and service access across different floor levels, limiting the comprehensiveness of current accessibility assessments.

2.3. Identification of facility locations and functional distributions

There are also critical challenges associated with the identification of 3D locations of facilities. Most studies rely on Points of Interest (POIs), Areas of Interest (AOIs), or land use parcels to define facility locations [50]. Among these, POI data are the most widely used in 15-minute city evaluations due to their higher spatial resolution and specificity in capturing the locations of individual services and amenities. POI datasets are available from a variety of commercial and open access sources, including volunteered geographic information (e.g., OpenStreetMap [34, 51]), government [52] and companies (e.g., SafeGraph [53, 54]). Despite their widespread availability and extensive spatial coverage, POI datasets often suffer from issues of incompleteness and uneven data quality [55, 56]. Moreover, not all urban services are consistently recorded as POIs. Some facilities may be missing because they are infrequently visited, recently relocated, or not formally registered. These omissions lead to the underestimation of facility counts and, consequently, the misrepresentation of local accessibility levels.

Recent efforts in building-level function inference have attempted to address some of the limitations in facility identification. Studies using street-level imagery and remote sensing data have made progress in classifying the functions of individual buildings, offering a more comprehensive understanding of urban functional composition [57, 58, 59, 60, 61]. The results of approaches have good performance in coverage, but they often rely on generalized and ambiguous classifications, such as "mixed-use", to represent the presence of diverse amenities within buildings. While the "mixed-use" label captures functional complexity at a broad level, it fails to reflect the specific composition and spatial arrangement of amenities across floors. For example, many makeup studios, photography studios, and other important amenities are located on non-ground floors within apartment buildings, which are calculated using large POI data in China [11]. Therefore, a key limitation is the lack of detailed information on the vertical distribution of facilities within buildings, both in POI datasets and in building function inference outputs. In the previous studies, the mixed-use effects have been considered in the traveling time estimation [31, 62].

In high-density urban environments, multi-story buildings often accommodate a mix of services, such as offices, restaurants, and retail stores, distributed across different floors. However, dominant occupants, such as offices, may occupy several floors and considerably larger floor areas than other services. As a consequence, analyses that rely solely on POI counts or building-level function classifications may misrepresent the true spatial density and vertical complexity of facilities, leading to inaccuracies in accessibility evaluations and spatial equity assessments in 3D urban settings.

2.4. Methods for calculating trip duration

Trip duration is primarily influenced by travel distance, and there are two main approaches used to measure distance and duration in 15-minute city accessibility evaluations. On the one hand, few studies rely on straight-line (Euclidean) distance to assess proximity [63]. These studies apply a buffer zone around the origin points, combining predefined distance thresholds to identify accessible facilities. While this method is computationally efficient, it oversimplifies real-world conditions, as road networks rarely follow direct paths, particularly in high-density urban areas.

On the other hand, most studies adopt network-based distance to accurately estimate travel time [64, 65]. This approach uses road network data to calculate the shortest path between origin points and destination facilities by GIS and route planning tools, like OpenTripPlanner [1], Mapbox [2] and 15min City Score Toolkit [66]. It has become a common practice in 15-minute city assessments [38]. Several digital mapping platforms also apply this approach, including CityAccessMap[3], X Minute City[4], and Aino[5]. By applying walking speed to the computed path length, more realistic travel times can be derived. However, with the emergence of 3D urban structures, both approaches share a common limitation: they neglect the vertical component of travel time. In high-rise buildings, residents spend a non-negligible amount

[1] https://github.com/opentripplanner/OpenTripPlanner
[2] https://www.mapbox.com
[3] https://www.cityaccessmap.com/
[4] https://research.uintel.co.nz/x-minute-city/
[5] https://www.aino.world/

of time navigating vertical circulation, including waiting for elevators, descending stairs, or transitioning between floors. Similarly, reaching destinations located on upper floors also entails vertical travel costs. This vertical time component is not accounted for in 2D models and leads to underestimation of actual travel durations. As a result, evaluations based solely on horizontal metrics may overstate accessibility levels and produce overly optimistic interpretations of 15-minute city performance in dense, vertical urban environments.

3. Materials and Methods

3.1. Study area

Our study area is Nanjing, a high-density city in China's Yangtze River Delta (Figure 1). We focus on the central area within the Roundabout Expressway, covering Gulou, Xuanwu, Qinhuai, Jianye, and Yuhua Districts and part of areas in Qixia and Jiangning Districts. As the core urban area, this region hosts the majority of Nanjing's population and encompasses diverse urban functions. Table 1, compiled using data from the Jiangsu Bureau of Statistics in 2020, details the population, area, and population density of the districts included in the analysis. The city's urban morphology is diverse, featuring historical districts with low-rise buildings especially in Gulou District, emerging high-rise CBDs, and well-developed university towns in Qixia and Jiangning Districts. These varied building typologies, designed to meet different urban living and production needs, result in a vertical heterogeneity of functions across building floors.

3.2. Multi-source urban data

This study uses multiple spatial datasets to support urban function and accessibility analysis. 2D building data with height from AMap provides building footprints and floor counts as the basic analysis unit[6]. POI data offers detailed facility points while AOI polygons from Baidu Maps represent areal-level urban function[7]. EULUC-China supplies parcel-level land use data for major cities, and a gridded

[6] https://amap.com
[7] https://map.baidu.com/

Table 1: Population, Area, and Population Density of Districts

District	Population	Area (km^2)	Population Density ($/km^2$)
Gulou	940,387	53.87	17,457
Qinhuai	740,809	49.15	15,072
Xuanwu	537,825	75.21	7,151
Jianye	534,257	80.94	6,601
Yuhuatai	608,780	133.20	4,570
Qixia*	987,835	390.00	2,533
Jiangning*	1,926,117	1,564.00	1,232

Note: * indicates that the population and area refer to the entire district, while only a portion of the district was used in this study.

GDP dataset helps assess socioeconomic accessibility inequality. The road network from OpenStreetMap is the proxy to measure the network distance[8]. These datasets are summarized in Table 2.

2D building footprints with height, referring to the ground projection boundaries of buildings, serve as a fundamental data source in our analysis. The footprints, along with their associated floor numbers provided by Gaode Maps, are considered highly reliable [68, 69]. Floors serve as the primary unit of analysis in our study.

POI data is our primary urban function data source for inference. As a fundamental geospatial dataset, POIs represent service facilities along with their location attributes. These points not only include names and geolocation coordinates but also often provide detailed floor or building information in the address, which is a critical element for our floor-level function inference. The dataset comprises 24 subtypes, and we used a total of 150,654 POI points to support our analysis.

AOI data, presented as polygonal subparcel-scale geospatial information, is used to represent urban functions within specific areas. We obtained AOI data from Baidu Maps, which categorizes urban functions into 11 distinct types. In total, we utilized 6,277 AOI polygons to ensure a comprehensive representation of urban functions

[8] https://www.openstreetmap.org

Table 2: Data sources used in this study.

Name	Description	Example	Provider
Building footprints	A building dataset containing polygonal footprints and associated floor numbers.		AMap
POI	A point-based dataset that records the geographic locations and attributes of various places of interest, such as schools, hospitals, and offices.		AMap
AOI	An area-level dataset representing functional zones (e.g., campuses, residential blocks, commercial complexes).	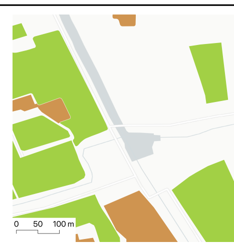	Baidu Map
EULUC-China	A parcel-level land use dataset for China, capturing detailed land use classification across multiple categories.	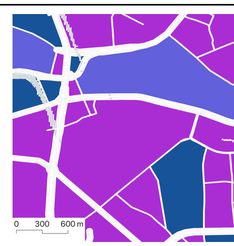	[67]
Road network	A vector-based road network dataset, providing multi-level road classifications (e.g., highways, arterial roads, local streets)for routing.		OpenStreetMap

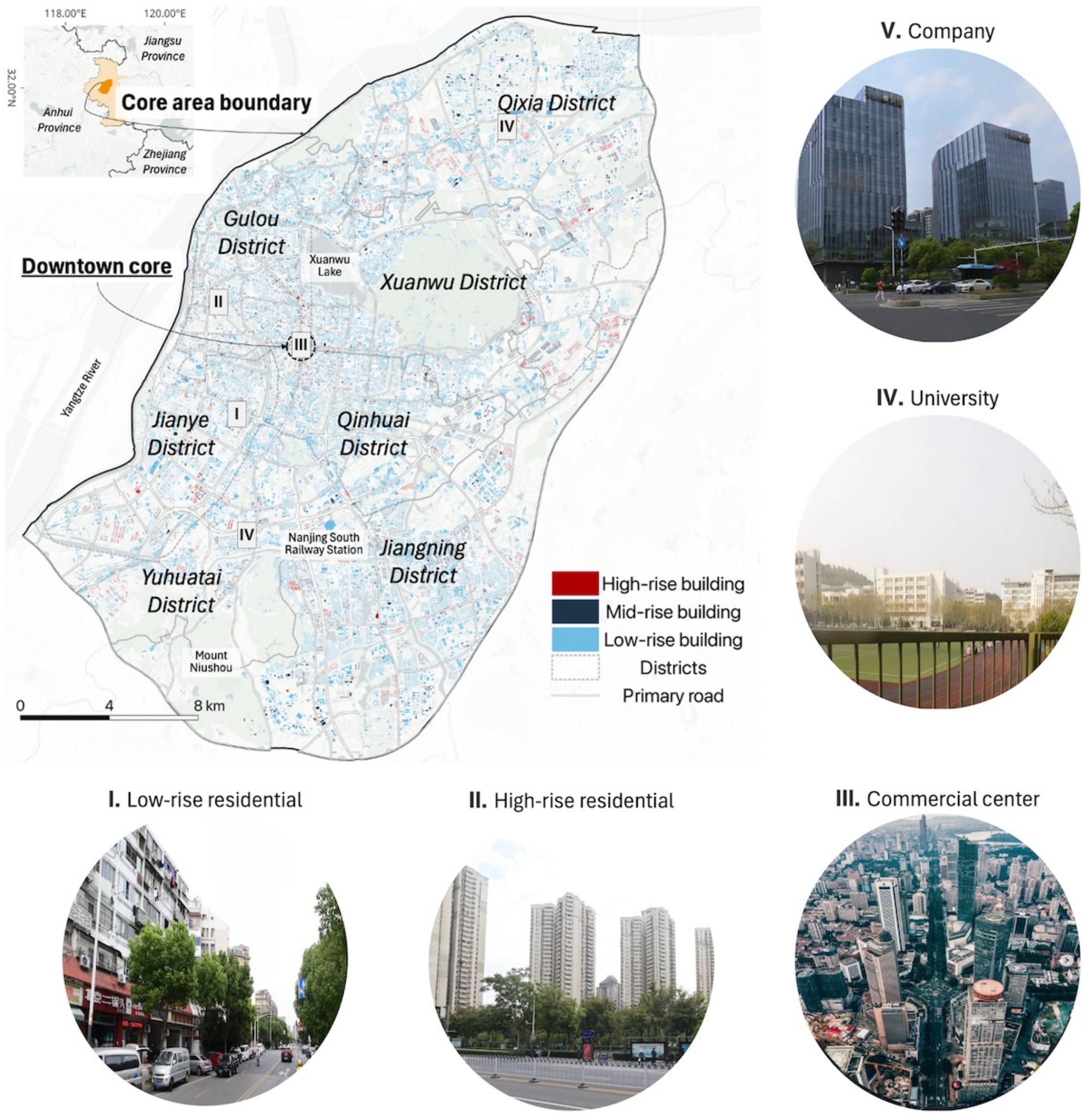

Figure 1: Study area – the core of Nanjing (China) , covering most of this diverse city's population and economy. Basemap: CARTO Map. Street view images: Baidu Map.

across the study area.

EULUC-China is a well-known, parcel-scale land use dataset covering major Chinese cities [67]. Its classification system divides land use into five primary types and twelve secondary types. This dataset has demonstrated reliable performance in validation and has been applied in various urban studies [70, 71].

We used spatially explicit gridded GDP data to assess accessibility inequality in our study [72]. This dataset employs an NTL-population-based method for socioeconomic disaggregation, covering over 60% of the global land surface. Its spatial resolution is approximately 30 arc-seconds (nearly 1 km).

3.3. Overview of Method framework

The research framework, introducing a holistic methodology for analyzing and assessing 15-minute city in 3D building environments, is structured into three steps, as illustrated in Figure 2.

Step 1: Mapping 3D functional composition of buildings (Section 3.4) We map the 3D functional composition of buildings using multi-source data (POI, AOI, and land use). We assign 2D POI locations to nearest buildings, extract 3D geolocations via natural language processing (NLP) and rule sets. Floors without direct POI data are filled using AOI and land use data, and we calculate the area ratio of each function per floor.

Step 2: Estimating 3D travel time (Section 3.5) We simulate 3D travel time from residential to amenities. Travel time is estimated by combining horizontal network-based distances (computed from the road network) with vertical travel time within buildings (e.g., elevator and stair usage), yielding a total 3D travel duration for each trip.

Step 3: Assessing 15-minute city (Section 3.6) We develop 3D 15-minute proximity indices at floor-level. It is used to evaluate overall 15-minute accessibility and spatial equality. Furthermore, we integrate urban form indicator to explore their relationship with observed accessibility patterns.

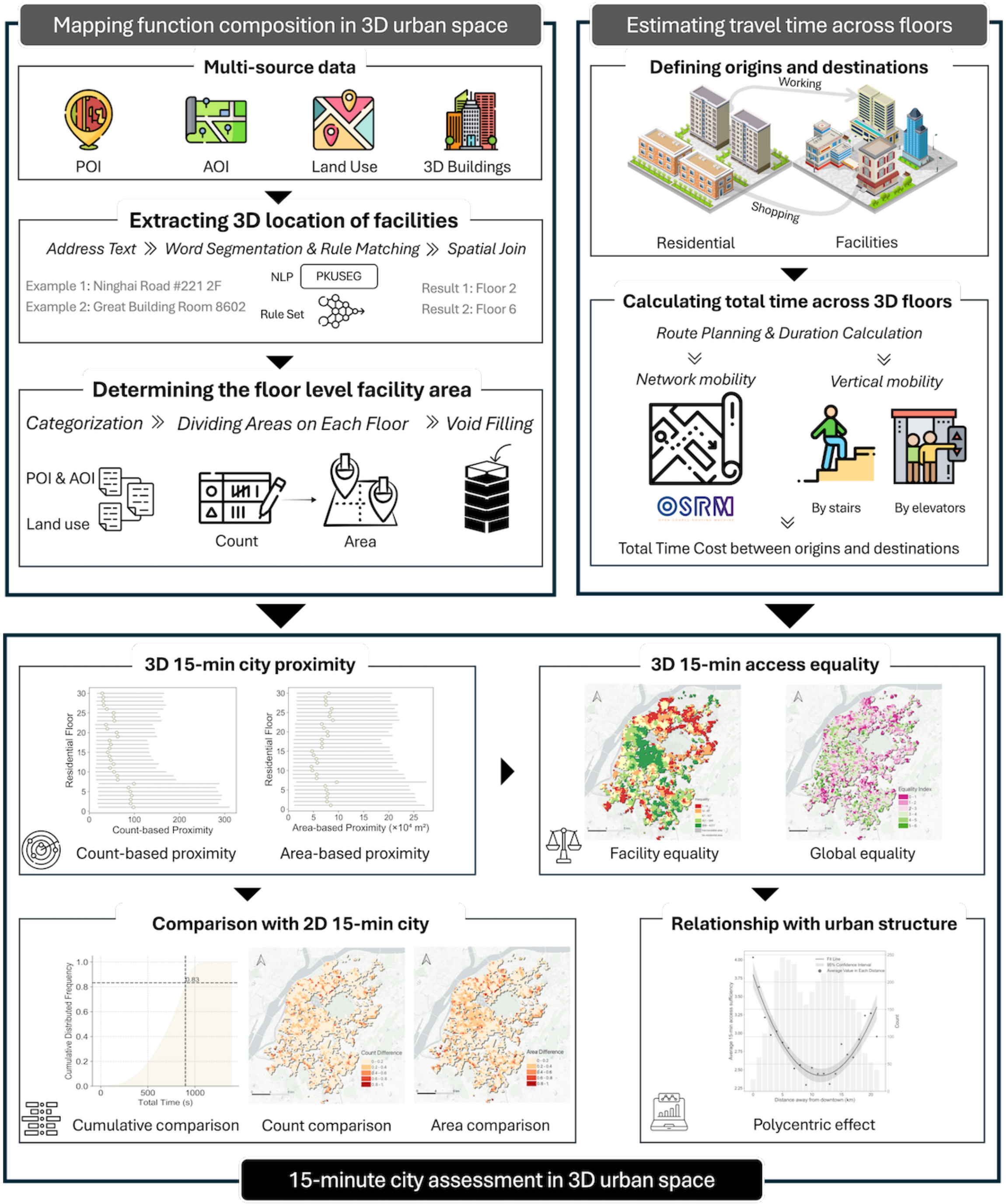

Figure 2: Overall workflow for evaluating the 3D 15-minute city by incorporating 3D distribution of amenities and vertical time cost.

3.4. Determining function composition in 3D buildings

Recognizing the spatial uncertainty of POI geolocations, where many points fail to intersect with actual building footprints, we further examined the spatial relationships between POIs and buildings to correctly allocate POIs to their corresponding structures. POI addresses often contain floor-related information, but the tokens used vary considerably due to inconsistent naming conventions. To accurately extract floor-level values, we developed a method that combines NLP with a rule-based parsing system. By fusing POI, AOI, and land use parcel data, we derived detailed, floor-by-floor functional compositions for individual buildings. We also evaluated the floor-level function accuracy by manual labeling with street view images and commercial POI platforms (Meituan [9] and Dazhong Dianping [10]).

Extracting 3D location of facilities. To resolve spatial misalignment between POI points and building footprints, we applied a spatial nearest-neighbor approach. For POIs that did not intersect any building polygon, we identified and assigned the nearest building using Voronoi tessellation. This step ensured that POIs were spatially allocated to their most probable building entity, enabling accurate linkage between textual floor information and 3D building models.

To ensure consistent text parsing, address strings were first standardized by removing whitespace, dashes, and punctuation, and by converting Chinese numerals to Arabic numerals. Special attention was paid to supplementary information enclosed in parentheses, which was extracted and preserved as additional attributes. After standardization, we employed the mixed segmentation mode of the PKUSEG NLP model to tokenize the address into meaningful components such as road names, lanes, building blocks, and units. We then searched for floor-indicating tokens and extracted the adjacent characters as potential floor values.

A hierarchical rule set was used to interpret these extracted details. If no floor-related tokens were found, the floor was assumed to be the first level (Floor 1). For cases containing a one- or two-digit number along with floor indicators, we checked for the presence of the letter 'B', which typically denotes a basement level. POIs

[9] www.meituan.com
[10] www.dianping.com

referencing basement floors were excluded from further analysis. Otherwise, the numeric value was assigned as the floor level. When a three-digit number appeared, we used the first digit as the floor indicator. In four-digit cases, the first two digits were extracted and compared against the known floor range of the associated building. If these digits fell within the building's floor range, they were accepted; otherwise, the second digit was used because we have observed that some of these addresses may have a lucky number in them (e.g., eight). This structured rule system allowed us to reliably extract floor values from diverse and often ambiguous address formats. To facilitate a better understanding of this approach, we show the pseudo code in Algorithm 1.

Determining floor-level function composition. The functional frameworks for POI and AOI differ from traditional land use classifications due to their finer granularity. To address this, we reclassified both POI and AOI types into a unified framework comprising seven major land use categories: residential, company, commercial, public service, education, medical, and recreation. The definitions of these categories are informed by land use classifications [67] and the work of Moreno et al. [13], as detailed in Table A.3. We excluded the transportation and greenspace categories from the land use dataset, as facilities such as bus stops and parks are typically not located within buildings and primarily serve to support accessibility rather than directly fulfilling daily needs. Although this filtering may omit certain facilities like railway stations, their limited role in everyday residential environments is unlikely to significantly affect the overall results. Using the reclassified data, we counted the facilities and calculated the ratio of each facility type on a floor-by-floor basis using POI data. This ratio serves as the basic composite function for each floor. Notably, due to incomplete floor information in the POI dataset, we implemented a strategy to fill void floors. Specifically, if a building is covered by AOI data, we assign the corresponding AOI type to that floor; if the building is only covered by the land use layer, we designate the floor based on the land use parcel type.

3.5. Calculating OD trip durations in 3D space

Defining the origins and destinations. Defining origins and destinations is a crucial step in accessibility analysis. In this study, we first designate the identified residential floors as origins and select facilities as destinations to reflect the realistic travel needs of residents. To eliminate unnecessary trips in our 15-minute assessment, we removed destinations located beyond a 2000 m buffer from the origins. After filtering, we generated the origin-destination relationships and stored them in an SQLite database.

Calculating total time among 3D floors. The duration in this study comprises two components: network time cost and vertical time cost. Network time cost represents the time spent traveling on the road network (i.e., the planar distance), which we calculated using the Open Source Routing Machine [73] on the OpenStreetMap network, assuming a walking speed of 5 km/h. This speed is widely used as it approximates the average pace across diverse population profiles and facilitates straightforward calculation [74].

Vertical time cost, on the other hand, accounts for the time required to traverse between floors whether by climbing stairs or using elevators. To estimate vertical time cost, we first classify buildings into two categories based on their floor counts. Buildings with seven or more floors are assumed to have elevators available, whereas those with fewer floors are considered to rely solely on stairs. For stair climbing, we set the average speed at 0.3 m/s referred by [75]. For elevator usage, we assume a speed of 1 m/s which referred by some commercial company data [76, 77], and we add an extra waiting time equivalent to the time the elevator would take to cover half the number of floors in the building. This combined approach provides a more realistic estimate of the total travel duration by capturing both the horizontal movement on the street network and the vertical movement within buildings. The expression of total time cost as Equation 1.

$$T_{\text{total}} = \frac{D}{5} \times 60 + \begin{cases} \frac{f \cdot h}{v_s \cdot 60}, & \text{if } F < 7 \quad \text{(stairs)} \\ \frac{(f + 0.5F) \cdot h}{v_e \cdot 60}, & \text{if } F \geq 7 \quad \text{(elevator)} \end{cases} \tag{1}$$

where D is the horizontal network distance between the residential building and the destination facility (in kilometers). F is the total number of floors in the building. f is the target floor number within the building that the individual seeks to access. h represents the height of a single floor, assumed to be 3 meters throughout the study. v_s is the vertical climbing speed when using stairs. v_e is the elevator speed.

3.6. 3D 15-minute city proximity and its equality assessment

Assessing count-based and area-based 3D 15-minute proximity. After calculating the total travel time for each origin-destination pair, we filtered out any trips with durations exceeding 15 minutes. Of the 96,587,581 pairs identified, 44,004,073 met this criterion and were retained for analysis. This step yielded a refined subset of origins, the residential floors, and their corresponding destinations that could be accessed within the desired time threshold. Within this dataset, we quantified Count-based proximity C_i as the total number of accessible facility floors from a given residential floor (Equation 2) and Area-based proximity S_i as the cumulative floor area of these accessible facility floors from a given residential floor (Equation 3).

$$C_{i,j} = \sum_j \delta \left(d(\text{residential}_i, \text{facility}_j) \leq 15min \right) \tag{2}$$

$$S_{i,j} = \sum_j A_j \cdot \delta \left(d(\text{residential}_i, \text{facility}_j) \leq 15min \right) \tag{3}$$

where $d(\text{residential}_i, \text{facility}_j)$ denotes the time spent from residential floor i to facility type j and A_j means the area of facility floor j. These indices mainly demonstrate the basic accessibility from the residential floor.

Measuring 15-minute city equality. Although the access proximity-based indices capture the potential opportunities available from facilities, they do not fully reflect access equality. For example, a sizable residential floor with many households might have access to some commercial floors within a small area. Yet, the cumulative facility floor area may still be insufficient for residents' needs due to the large number of households. To address this, we introduce the floor-level access equality (AE) metric in Equation 4, which evaluates whether the accessible floor area meets the demands of the residential floor. To understand the local heterogeneity, we also aggregated the floor-level AS to the hexagon level by calculating the median value.

Given the heterogeneity in accessibility distribution among different facility types, using absolute values alone to evaluate the achievement of a 15-minute city presents challenges. To overcome it, we employed a ranking weight on a city-wide scale that normalizes the differences between facility types. Specifically, we ranked the accessibility equality for each hexagon unit by assigning the highest value a rank of

1, with the remaining values ranked in descending percentile order as Equation 6. By summing these rank ratings, we derived a global access equality index in Equation 7. This approach not only standardizes the assessment across various facility types but also facilitates a more equitable comparison of regions, which helps us to discover and understand the regions that should be optimized.

$$AE_{i,j} = \frac{S_{i,j}}{POP_i} \tag{4}$$

where $AE_{i,j}$ denotes the area accessibility or service level of type j on floor i and POP_i is the population residing on floor i.

$$POP_i = \frac{A_i}{HouseArea_{per}} \tag{5}$$

where A_i is the total floor area of floor i (m^2), and $HouseArea_{per}$ is the per capita living area, assumed as 40 m^2/person referred by Nanjing Municipal Bureau of Statistics.

$$\mathrm{rank}_h = \mathrm{Rank}\left(\mathrm{median}\left\{AE_i \mid i \in h\right\}\right) \tag{6}$$

where rank_h is the descending rank assigned to hexagon h based on the median AE_i values of floors within it.

$$E_{\mathrm{access}} = \sum_{h=1}^{H} \frac{1}{\mathrm{rank}_h} \tag{7}$$

where H is the total number of hexagonal spatial units in the study area, and E_{access} is the global accessibility equity indicator, computed as the inverse-rank-weighted sum across all hexagons. A higher E_{access} indicates greater sufficiency and spatial balance in access to facilities.

4. Results

4.1. The composition of functions in 3D buildings

We determined the facility type and floor-level area by extracting the 3D locations of POIs from address texts and supplementing missing data using AOI and land use information for Nanjing. Figure 3 illustrates the composition of facilities by floor below the ninth story. In the left subplot, we aggregate and display the total facility areas across different floors, while the right subplot presents the corresponding proportions. The results show that the lower floors (Floors 1 to 3) are primarily occupied by company, commercial, and residential functions, which cover the largest share of space. Although the total area allocated to facilities decreases with building height, residential functions consistently dominate the composition, with their proportion increasing on higher floors. Educational, medical, and public service functions are distributed across all floors but represent a relatively small share. Commercial facilities, such as grocery stores and restaurants, are concentrated on the first floor to support daily needs, explaining the higher proportion at lower levels. In contrast, commercial space becomes less prevalent on upper floors, whereas the share of educational functions remains relatively stable. This pattern may reflect the spatial characteristics of institutions such as universities and research centers that typically occupy multiple stories, resulting in a consistent vertical presence.

The performance of floor-level functions was evaluated using four sampling areas (Figure D.16). The confusion matrix (Figure D.17) illustrates the distribution of prediction errors across categories. Overall accuracy, precision, and F1 score were adopted as key indicators. As summarized in Table D.4, the results demonstrate generally high reliability, with accuracies ranging from 0.85 to 0.97 across the four blocks.

4.2. Evaluation of 3D 15-minute access proximity

To provide an intuitive understanding of count-based and area-based proximity in a 3D urban context, we selected two representative buildings to illustrate the vertical variation in accessibility. Figure 4(a) presents the proximity indices for a ten-story residential building located within a typical residential block. According to our model, travel from the 10th floor to ground level takes approximately 45 seconds. This vertical time cost leads to lower accessible counts and areas for most facility types on higher floors compared to the first floor, with the exception of public services. Notably, accessibility to company-related facilities exhibits a more pronounced decline, likely due to their greater average distance, which amplifies the effect of ver-

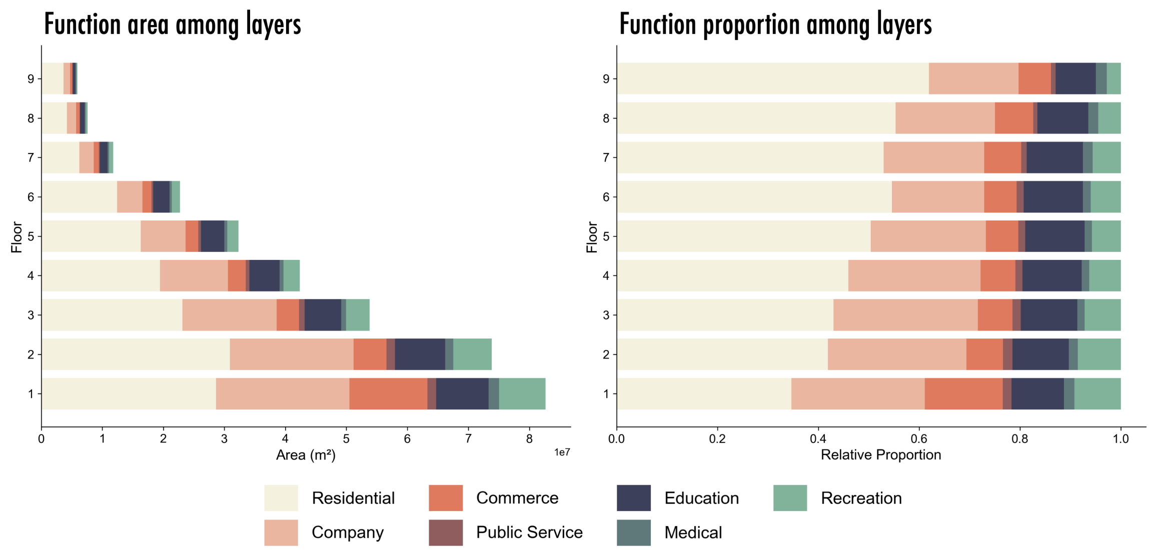

Figure 3: The composition of floor-by-floor facilities. The left panel shows the total area (m^2) of each functional type across floors, while the right panel presents their relative proportions per floor.

tical travel time. The reduction in proximity for other facility types suggests that residents on higher floors may have fewer accessible options within the same time threshold, highlighting significant vertical disparities in 15-minute accessibility for residents. Figure 4(b) presents a representative mixed-use building in a downtown area, along with its corresponding street view image. We calculated both the number of times each floor served as a destination and the average travel time to those destinations. The ground floor hosts multiple facility types, including offices, commercial services, educational institutions, medical facilities, and recreational spaces. This configuration suggests that a single residential floor within the building can access several types of destinations without exiting the structure. According to the analysis, the first floor demonstrates significantly higher accessibility compared to the 10th and 20th floors, primarily due to shorter vertical travel times and the diversity of available facilities.

We also conducted a comprehensive statistical analysis of count-based and area-based proximity for all residential floors within 15-minute threshold, as shown in Figure 5. Figure 5(a) summarizes the variations in count-based proximity across different facility types. According to the boxplots, the high median number of acces-

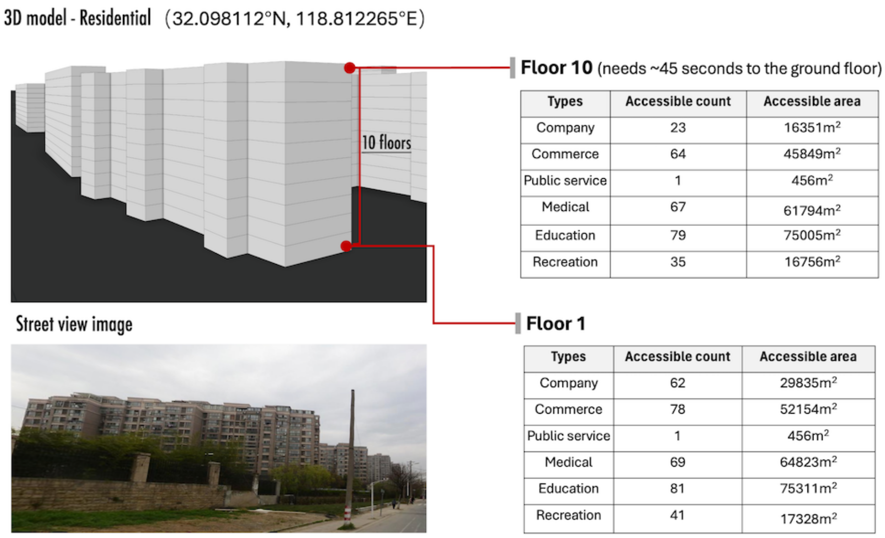

Floor 10

Types	Accessible count	Accessible area
Company	23	16351m^2
Commerce	64	45849m^2
Public service	1	456m^2
Medical	67	61794m^2
Education	79	75005m^2
Recreation	35	16756m^2

Floor 1

Types	Accessible count	Accessible area
Company	62	29835m^2
Commerce	78	52154m^2
Public service	1	456m^2
Medical	69	64823m^2
Education	81	75311m^2
Recreation	41	17328m^2

(a) A selected residential with 10 floors.

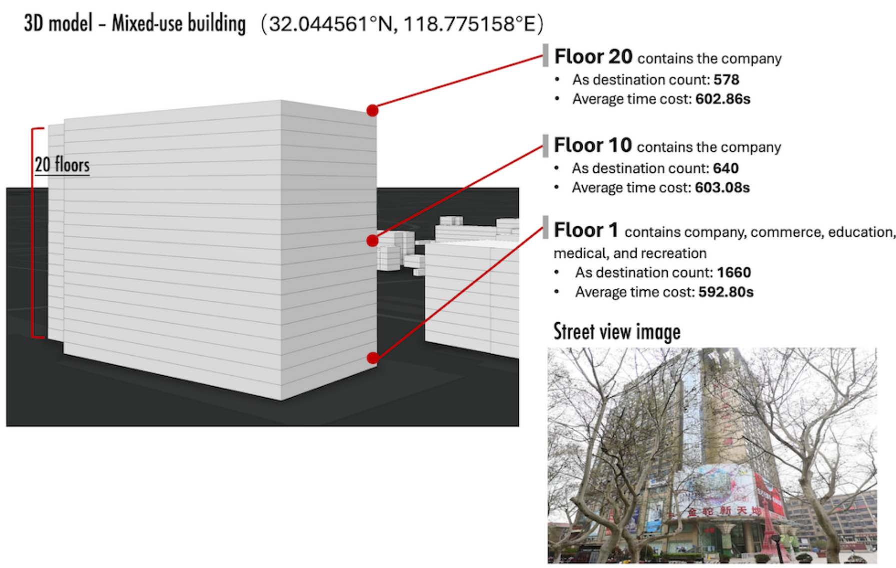

(b) A selected mixed-use building with 20 floors.

Figure 4: The count-based and area-based proximity of selected buildings. Source of street view image: Baidu map.

sible facilities for company and commercial functions suggests that most residential floors are within reach of multiple such facilities under the 15-minute threshold. In contrast, the proximity distributions for educational and public service facilities are more dispersed, with educational facilities exhibiting a particularly long-tailed distribution. This indicates their strong spatial concentration in certain areas and relative scarcity in others. Medical and recreational facilities show lower and more variable accessibility overall. The distribution patterns of area-based proximity, illustrated in Figure 5(b), are generally consistent with those of count-based proximity. In terms of accessible area, company, commercial, and educational facilities again exhibit higher values. Notably, public service, medical, and recreational facilities exhibit smaller average accessible areas, but with greater variability. It implies that although these facilities are limited in number, some districts still benefit from a relatively large supply of service space.

Figure 6 shows the vertical variation of count-based proximity across residential floors below the 30th level, within a 15-minute travel threshold. Overall, both the number and area accessibility of most facility types tend to decline with increasing floor height, suggesting that residents on higher floors generally have access to fewer facilities and smaller service areas within the time constraint. Among all facility types, commercial, public service, and medical facilities show the most substantial decrease in accessibility as floor height increases in count and area access. Notably, for area-based proximity in Figure 7, accessibility to company and commercial facilities initially declines with floor height but shows an increase above the 20th floor.

4.3. 3D 15-minute access equality and the relationship with urban form

In this phase of the analysis, we implemented a two-level assessment approach. First, the index was computed on a floor-by-floor basis. Second, to capture broader spatial patterns of the 15-minute city, the floor-level results were aggregated using the H3 geospatial indexing system at resolution level 9, corresponding to an average hexagonal area of approximately 0.105 km^2.

Figure 8 presents the spatial distribution of 15-minute access equality for six categories of facilities. The maps display the median access equality within each hexagon, using an equal-interval classification. Overall, Company and Commerce fa-

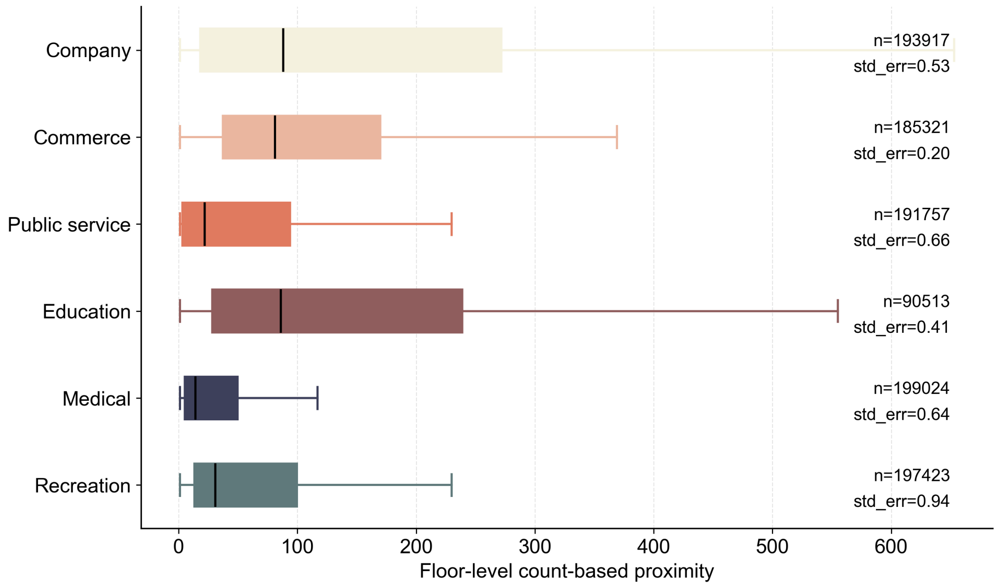

(a) Distribution of count-based proximity

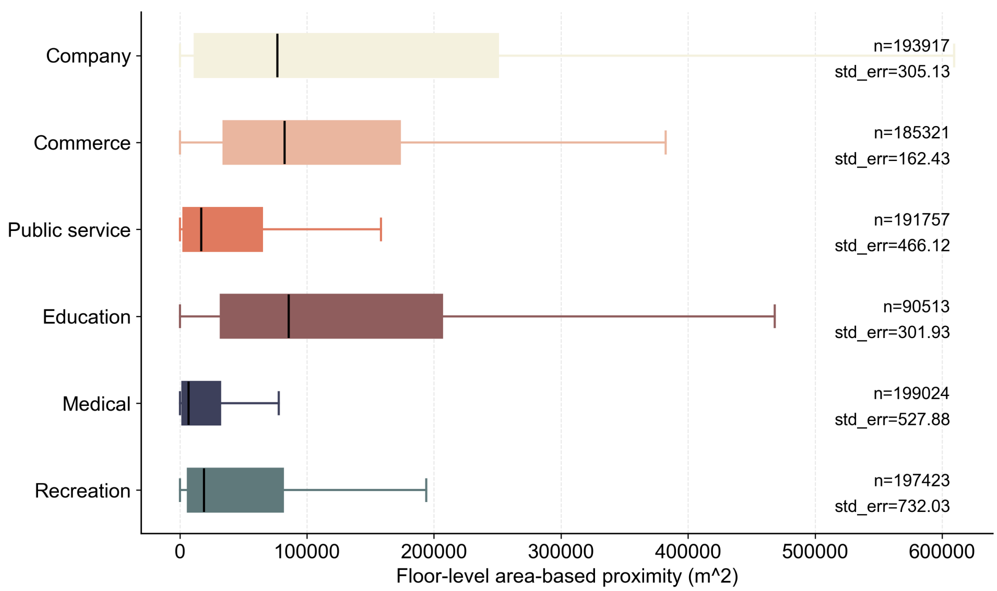

(b) Distribution of area-based proximity

Figure 5: Distribution of count-based and area-based proximity. Boxes represent the IQR, with medians and whiskers shown. Sample size and standard error (std_err) are annotated.

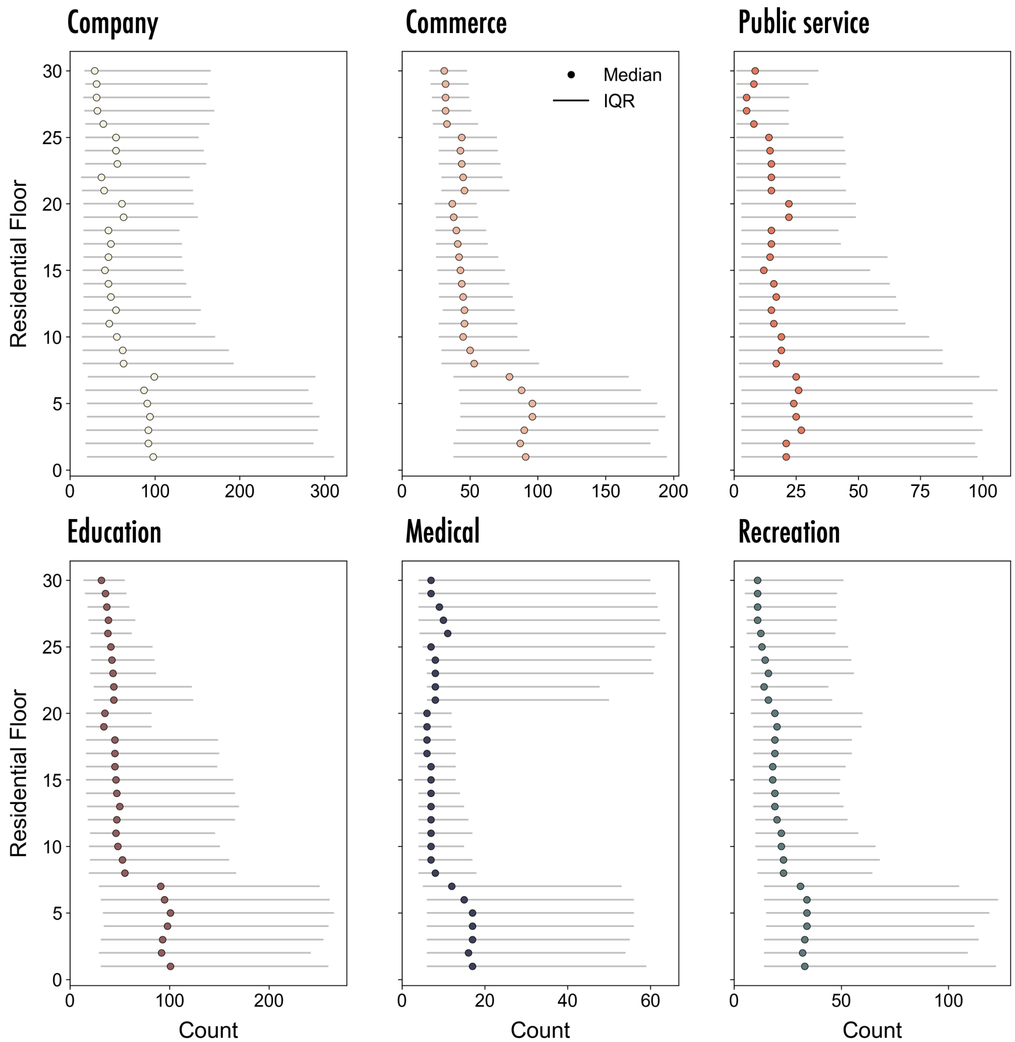

Figure 6: Floor-by-floor count-based proximity. This figure illustrates the proportion of floors that achieve 15-minute accessibility based on the number of accessible facilities. Dots represent the median count-based proximity values for each floor, while lines indicate the interquartile range (IQR).

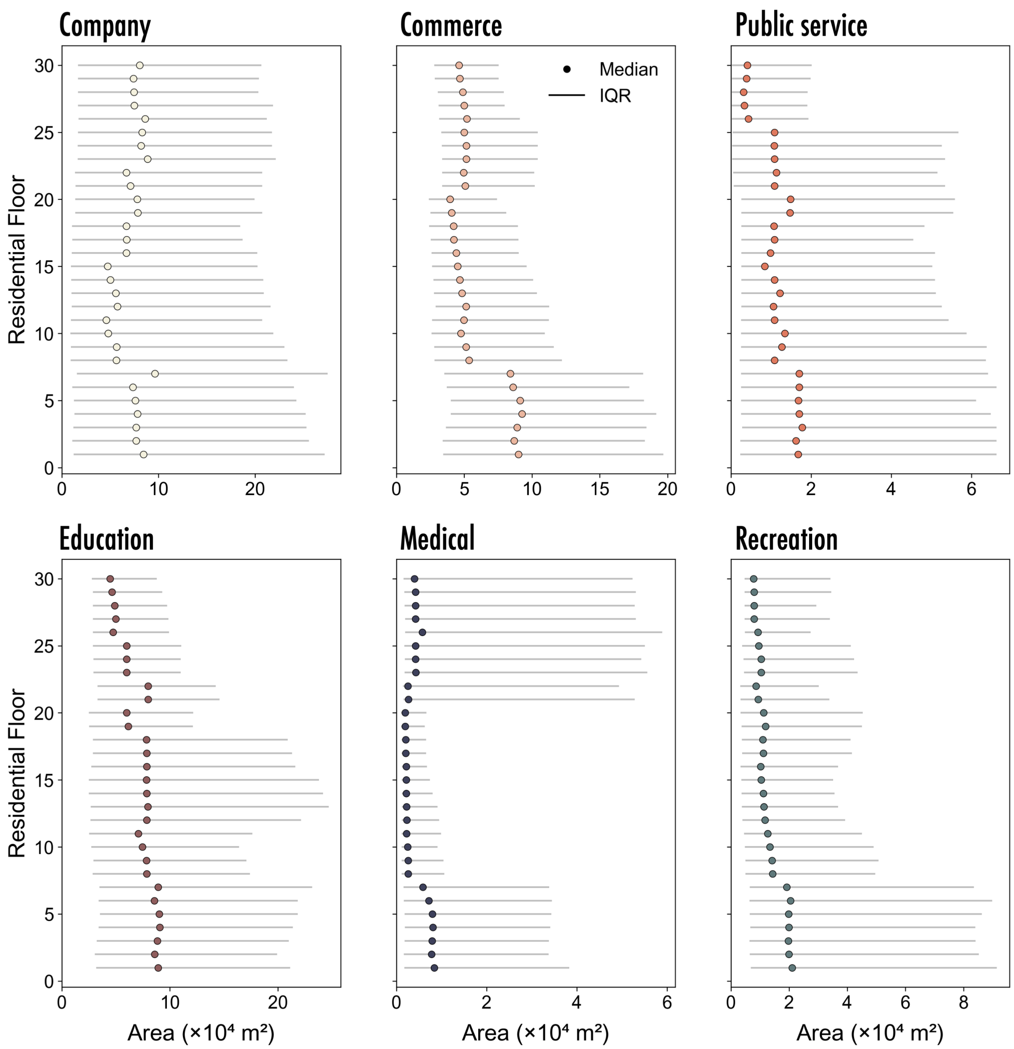

Figure 7: Floor-by-floor area-based proximity. This figure shows the proportion of functional area that can be reached within 15 minutes from each floor level. Dots represent the median area-based proximity values for each floor, while lines indicate the interquartile range (IQR).

cilities exhibit relatively high equality, suggesting a more balanced spatial coverage. In contrast, Public service, Education, Medical, and Recreation facilities show pronounced spatial disparities, particularly in urban fringe and southern areas, where red clusters highlight significant access inequality.

Using a rank-weighted method, we derived a composite measure of 15-minute access equality encompassing six types of urban facilities, as illustrated in Figure 9. Spatially, the urban core generally exhibits high equality, reflecting a relatively balanced distribution of services and minimal differences in accessibility across residential floors. To illustrate this, we examine a high-rise residential building (30 floors) near the downtown area, highlighting vertical variations in access equality across different destination types in Figure 9. In contrast, urban fringe areas, particularly in the southwestern and northern parts of the city, show distinct clusters of low equality. These patterns indicate that the multifunctional service capacity within the 15-minute walksheds in these regions is relatively weak, often characterized by either a scarcity of resources or a spatial over-concentration in a limited number of locations.

Figure 10 shows the relationship between the 15-minute access equality index and the distance of the region from the downtown to reveal the intrinsic link between the spatial structure of the city and the equity of services. The results reveal a clear 'U-shaped' relationship between service accessibility equality and distance to the city center. Notably, a marked decline in the equality index is observed within the intermediate belt, approximately 8 to 14 km from the city center, which indicates heightened disparities in service accessibility in this zone. This pattern is shaped by various factors, including the stage of urban development, geographic barriers (lakes, mountains and railway station) and the degree of functional land-use mixing. The intermediate area serves as a transition zone between older residential neighborhoods, newer development zones, and fragmented infrastructure systems, resulting in uneven service distribution and notable differences in access among residents. In Nanjing, natural and artificial geographical barriers such as Xuanwu Lake, Zhongshan Mountain National Park, and Nanjing South Railway Station have significantly influenced the spatial configuration of both the road network and built environment. Populations residing in proximity to these barriers often face reduced

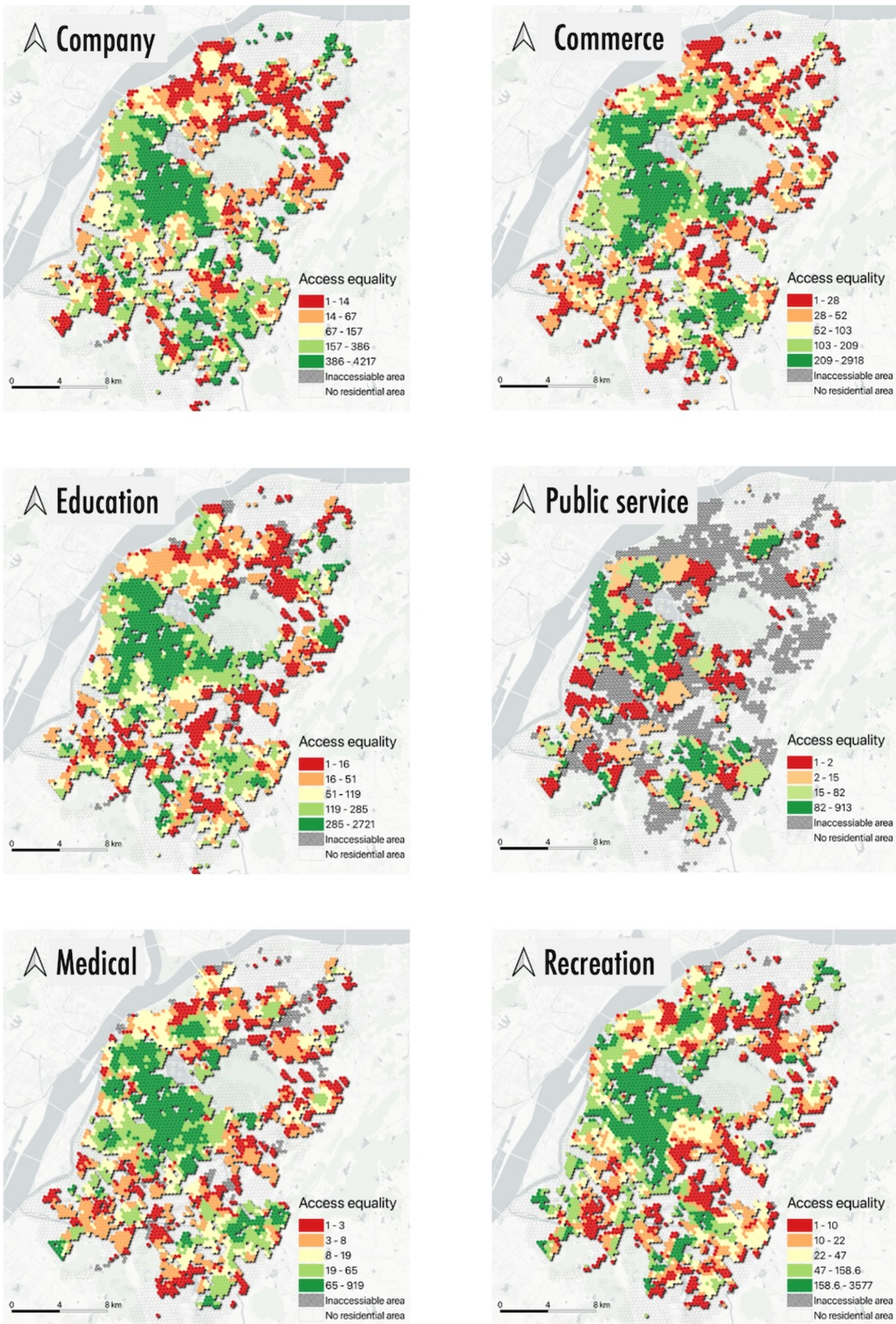

Figure 8: Spatial equality of 15-minute proximity across facility categories. Green represents high equality, while red denotes lower equality. Hexagons with black diagonal stripes indicate areas with no accessible facilities within 15 minutes, and grey areas are non-residential.

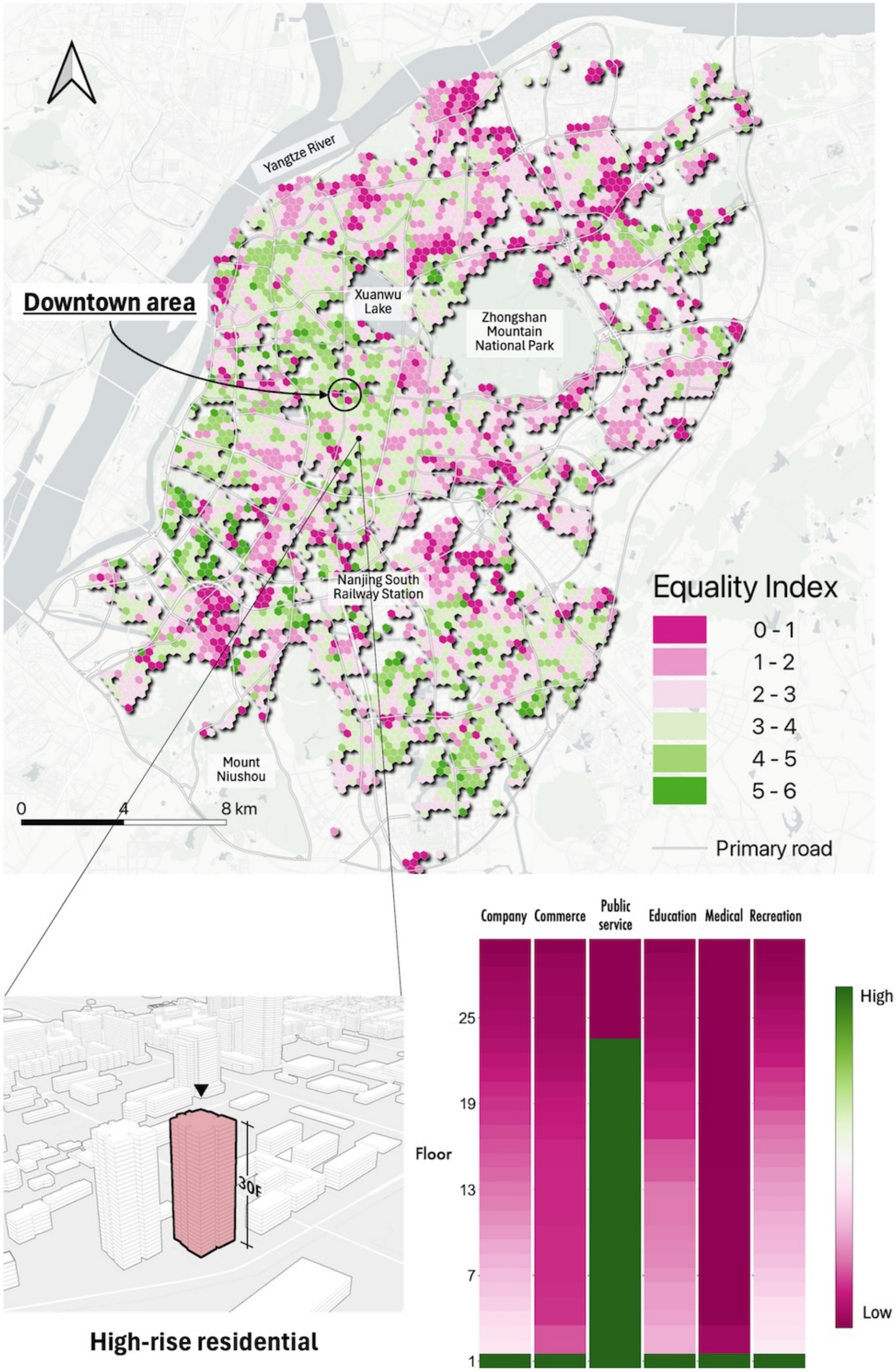

Figure 9: Map of overall 15-minute access equality. Purple denotes areas with lower levels of access equality, while darker green highlights areas with higher levels. Insets show a featured high-rise residential (left) and floor-level variations across functions (right).

accessibility and lower levels of service equity. The observed "U-shaped" pattern can also be interpreted through the lens of polycentric urban development theory. In principle, polycentric structures aim to enhance the spatial balance of services by establishing multiple sub-centers, thereby improving accessibility in peripheral and underserved areas. Between 2011 and 2020, the concept of polycentricity was formally incorporated into Nanjing's master plan [78]. However, the observed spatial equalities suggest that the functional realization of polycentric planning remains uneven. In Figure 11, we reclassified the 15-minute access equality according to four GDP classes, which reveals clear differences between groups. Figure C.15 shows the spatial distribution of GDP in Nanjing. Units in the higher GDP categories tend to exhibit higher levels of equality, while lower GDP categories show wider variability and generally lower equality scores. It is particularly evident in low-GDP areas, where a large number of samples show low index values, reflecting significant disparities in service accessibility and considerable internal variation. These findings underscore an association between economic development and the equity of urban service accessibility.

5. Discussion

5.1. Comparison with the traditional approach (2D 15-minute trips)

Figure 12 presents the cumulative distribution of actual travel time for a set of 15-minute trips initially identified using 2D accessibility, with subsequent adjustment for 3D spatial factors. The results indicate that incorporating 3D spatial generally increases actual travel durations across all facility types. Specifically, only approximately 83% (Company), 86% (Commerce), 86% (Public service), 87% (Education), 89% (Medical), and 89% (Recreation) of the trip pairs identified as accessible under 2D conditions remain within the 15-minute threshold when 3D factors are considered. This demonstrates that a subset of trips which deemed accessible in conventional 2D analysis in fact exceed the time limit once vertical travel costs are included. Notably, the decrease of public such as public services, education, and medical care may reflect their relatively limited spatial distribution, even though these facilities are essential for daily life.

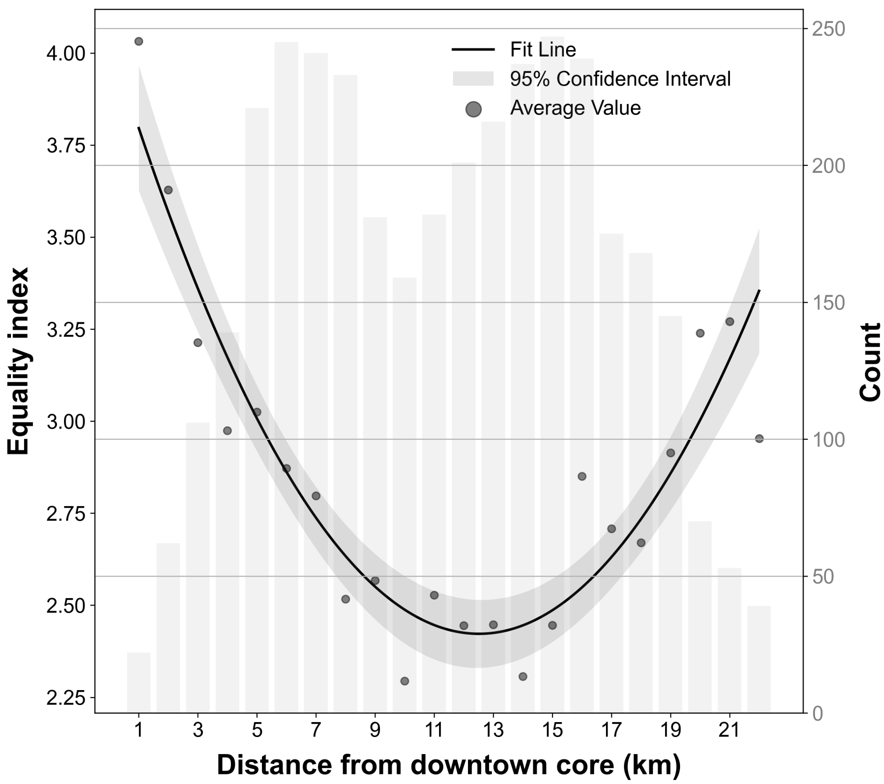

Figure 10: Relationship between 15-minute access equality and distance to downtown. The horizontal axis represents the Euclidean distance from the city center, while the vertical axis shows the average equality index, where higher values indicate more equitable access. The black solid line denotes the fitted trend curve, the grey shaded band indicates the 95% confidence interval, and the background bar chart displays the number of H3 hexagonal cells within each distance band.

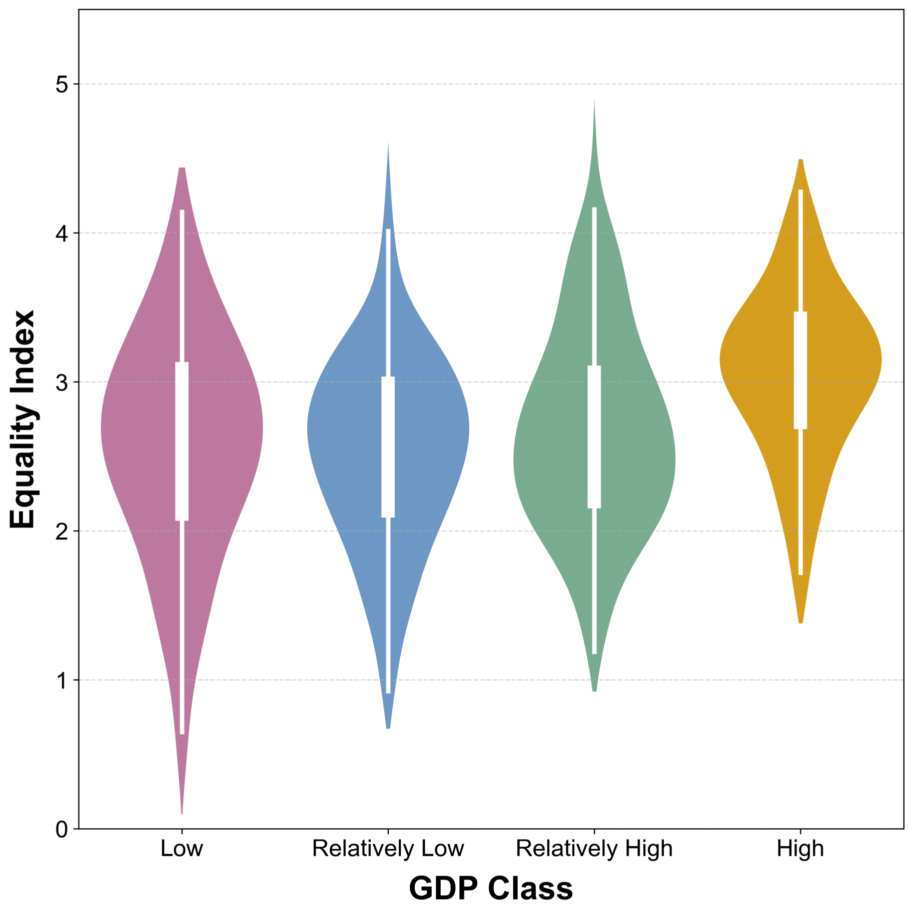

Figure 11: Distribution of 15-minute access equality across GDP levels. The violin plots show the distribution of equality index values grouped by GDP class. Wider sections indicate higher concentration of observations, while the embedded box plots display interquartile range.

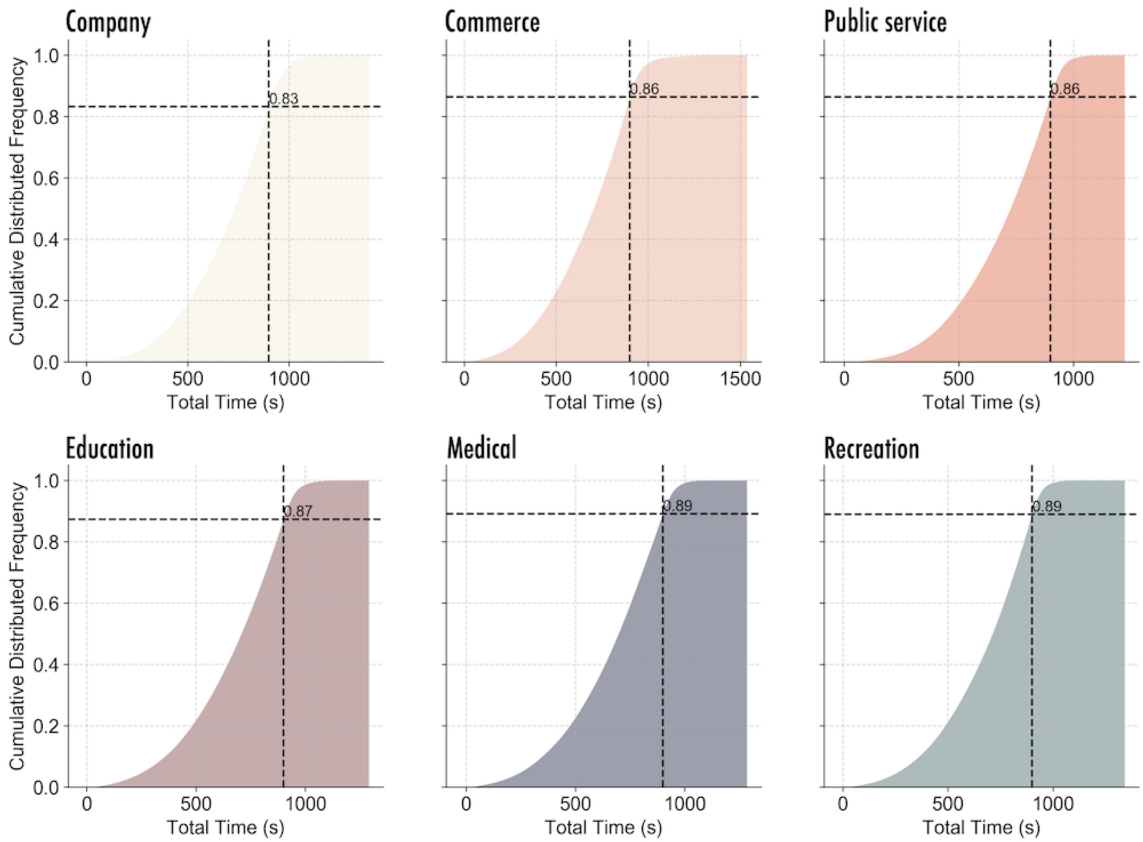

Figure 12: Cumulative distribution frequency of trip durations to compare the difference of 2D and 3D trips in travel time cost. A vertical dashed line marks the 15-minute threshold, allowing the cumulative percentage of qualifying trips to be visualized.

Figure 13 illustrates the spatial distribution of the proportional differences between 2D and 3D assessments for different facility types, across both count-based and area-based proximity dimensions. Color gradients represent the magnitude of change, with larger values indicating greater overestimation of actual service accessibility under the 2D evaluation, due to the exclusion of vertical travel time. The two types of indicators show relatively consistent spatial distribution characteristics, with the difference values concentrated between 0 and 0.2 in most areas. Notably, in certain central and peripheral urban zones a substantial number of cells show difference values exceeding 0.4. This highlights the significant influence of vertical accessibility on proximity assessments, particularly in high-rise environments.

On the one hand, regrading the count-based dimension as shown in Figure 14, facility types such as public services, education, and medical care exhibit prominent deviations in multiple areas. This suggests that vertical travel constraints may considerably affect the identification of accessible facility points. On the other hand, the area-based dimension Figure 14 reveals broader and more obvious variations, especially in the company, commerce, and public service categories, where high-difference clusters are more spatially concentrated. These patterns indicate that the service area of facilities is more sensitive to vertical access limitations than the number of accessible facilities.

5.2. Implications of vertical 15-minute city planning

There are two key implications of vertical 15-minute city planning, spanning both policy and design with opportunities and challenges. From a policy perspective, the vertical 15-minute city represents an extension and evolution of long-standing urban planning paradigms such as the compact city, the self-containment city, the polycentric city, and the inclusive city. An important insight from our analysis is the need to incorporate mixed-use development in both vertical and planar dimensions when planning for 15-minute city. Although the 15-minute threshold serves as a standard for classifying accessibility, our findings show that a substantial share of trips deemed accessible under 2D models exceed this threshold when vertical travel time is considered. This underscores the limitations of 2D assessments in high-rise contexts and the importance of systematically integrating vertical spatial factors into

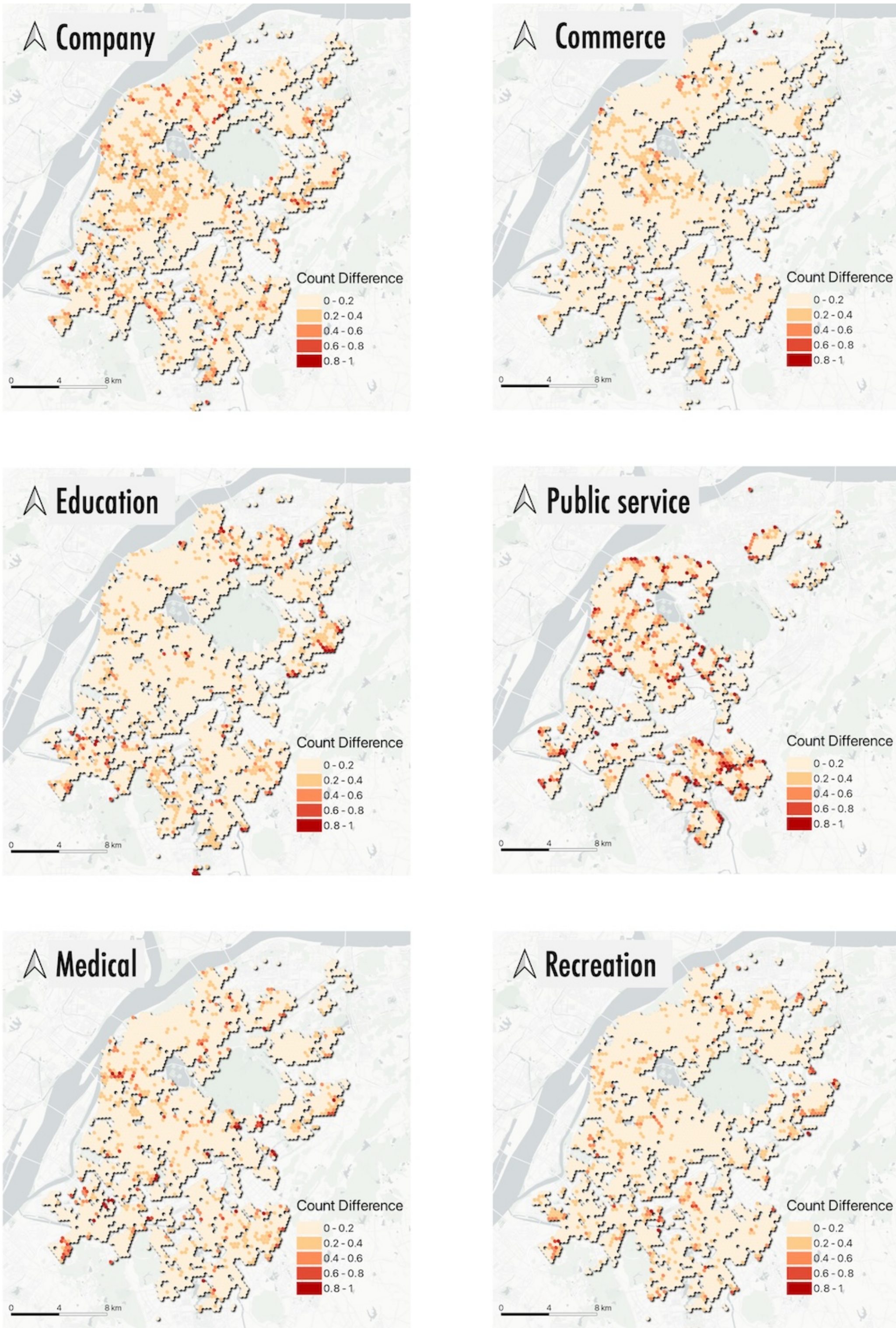

Figure 13: Ratio of count-based proximity differences before and after vertical travel time adjustment. Darker colors indicate larger differences between the two scenarios.

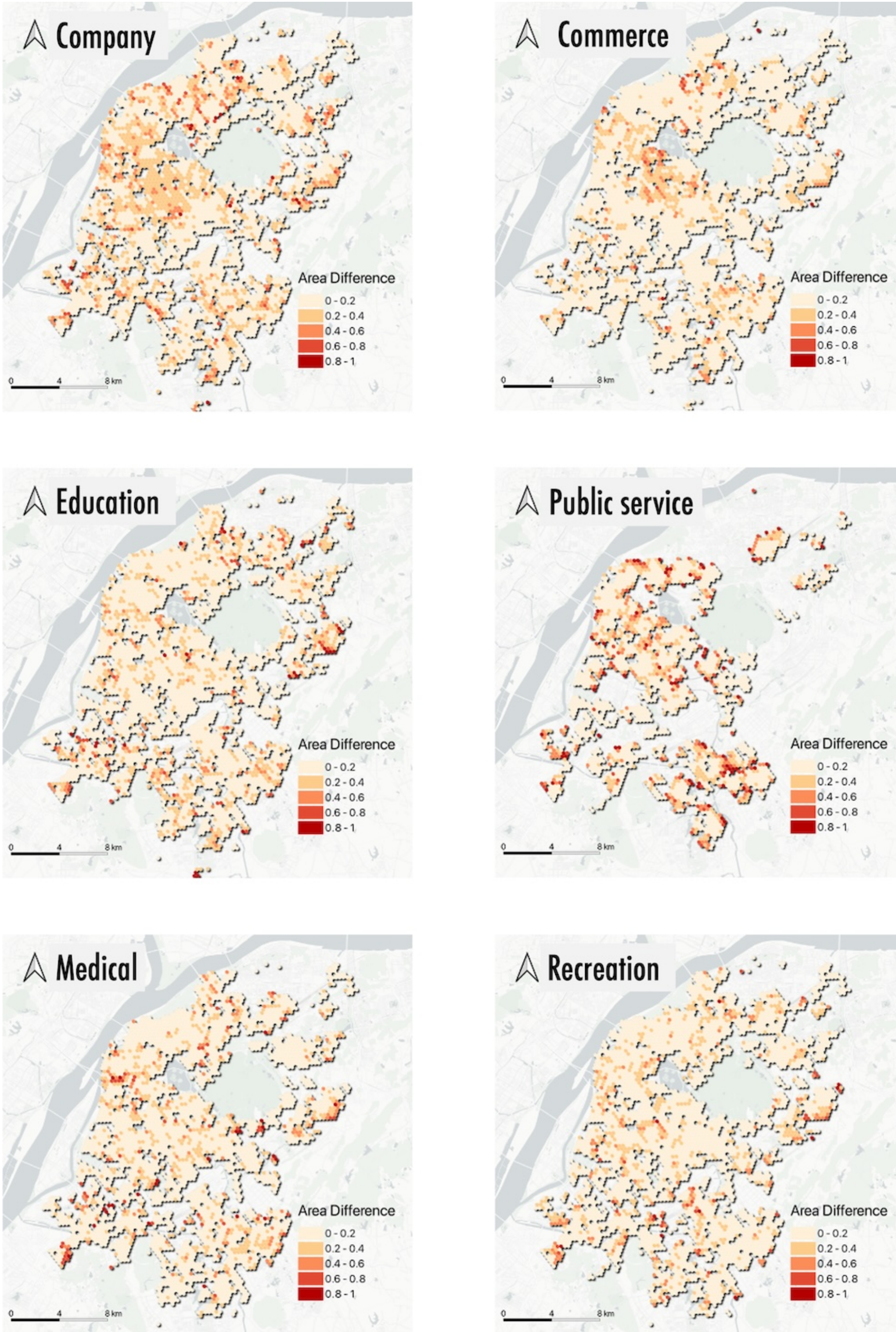

Figure 14: Ratio of area-based proximity differences before and after vertical travel time adjustment. Darker colors indicate larger differences between the two scenarios.

accessibility evaluations. Interestingly, while residents in high-rise housing generally require more time to reach a limited number of facilities, this limitation can be mitigated in compact and densely developed buildings where functional spaces are vertically mixed and efficiently distributed across multiple floors. Such configurations allow various services to be accessed within the same building or compact building cluster, thereby enhancing internal accessibility and supporting the realization of 15-minute living and self-containment city in vertical urban environment [79].

From a horizontal spatial perspective, polycentric planning is often adopted to improve accessibility by decentralizing services [80]. This outlook of the concept coincides with the 15-minute city. Yet, its current application may not fully address the needs of residents in transitional zones between urban cores and peripheral areas, where service availability can be uneven. Our findings point to the potential of extending polycentric strategies to incorporate vertical and social considerations. Embedding everyday services, particularly those related to welfare and care, within high-rise, mixed-use developments can help improve access for underserved communities [7, 10]. By aligning vertical design with social needs, cities can advance a more inclusive version of the 15-minute city that supports livability, fairness, and everyday well-being for all. Inclusiveness, a central concern of the 15-minute city, also requires targeted interventions in existing urban environments. For example, upgrading elevators and reorganizing service layouts in older housing estates to reduce vertical travel time, particularly for elderly and disabled residents, which helps and promotes to create a livable environment for vulnerable populations.

From the design perspective, it is essential for planners and architects to rethink the utilization of vertical space within the 15-minute city concept. Frequently visited but limited-number amenities should be concentrated on the ground or lower floors to enhance accessibility and reduce unnecessary vertical travel. At the same time, the introduction of internal public space networks, such as sky bridges, shared podiums, and elevated walkways, can connect different floors and adjacent buildings, thereby minimizing repeated elevator use, shortening waiting times, and easing circulation within dense clusters. Our results reveal a rapid decline in accessibility to public services, education, and medical facilities with increasing floor. Beyond mobility, embedding welfare and care facilities such as senior centers, daycare services, and basic healthcare clinics directly into high-rise, mixed-use developments can strengthen social support systems. In doing so, vertical design not only optimizes movement but also ensures that essential services are integrated into residents' everyday environments, supporting inclusivity and well-being in high-density urban contexts.

5.3. Limitations and future directions

The coverage and accuracy of the datasets used are critical to the reliability of our findings. This study integrates multi-source geospatial data to investigate the vertical distribution of urban facilities for generating a database to assess the 3D 15-minute city. While the datasets, sourced from various urban data platforms, provide detailed spatial representations, we acknowledge certain limitations that may cause results' uncertainty. First, POIs served as the primary data source for identifying floor-level facility composition. Although POI addresses contain rich semantic cues about 3D locations, and we employed a combination of NLP and rule-based parsing to infer floor information, some addresses lacked explicit floor references. In such cases, we defaulted the floor assignment to the first floor, which may have led to an underestimation of the degree of vertical functional mixing and the vertical component of travel time. However, our result may underestimate the 3D 15-minute city achievement degree due to the uncertainty of the POI address presentation. Second, discrepancies among data sources may introduce inconsistencies, particularly in facility classification schemes. In this study, we adopted a generalized classification framework, merging categories into seven broad types (e.g., education, public service). To fill these gaps, we relied on land use parcels, which offer broader but less detailed classifications. This approach introduces some degree of overgeneralization, potentially mixing distinct facility types. Fine-grained distinctions, such as primary schools, high schools, and universities, were not preserved due to missing values in land use data. However, it was a trade-off to support large-scale analysis of 15-minute accessibility in a high-density urban context. In this era of big data, we aim to integrate more comprehensive POI datasets with higher spatial coverage and more detailed address structures in the future. This will allow for more precise modeling of vertical facility distribution and finer differentiation of facility types, thereby improving both the accuracy and applicability of 3D proximity assessments in 15-minute city assessment.

Scaling our methodological framework to other cities for assessing the vertical 15-minute city remains an important direction for future work. Notably, extending this methodology to other cities presents both challenges and opportunities. Our framework provides a holistic workflow, ranging from data preprocessing to vertical 15-minute city assessment. This method includes eliminating spatial location bias in POIs, automatically identifying the floor information of amenities, and calculating floor-level access equality under the 15-minute city concept. The core idea of this framework is transferable to other cities, provided that similar types of data are available. However, in some Global South cities, there may be insufficient 3D spatial data and incomplete information on amenities, particularly in areas with informal settlements. Although various footprint-level building height datasets have recently emerged [81], the absence of detailed 3D amenity data remains a barrier. Even in developed countries with comprehensive spatial datasets, challenges remain in harmonizing heterogeneous data sources, maintaining temporal consistency, and ensuring comparability across different urban forms. Meanwhile, the intensity of effects that is introduced by vertical dimension may vary in magnitude across different types of X-Minute Cities (e.g., 10-, 20-, and 30-minute cities) and diverse urban form. Moreover, changes in accessibility distances may generate both positive and negative societal impacts in sustainable urban management worldwide. On the one hand, denser accessibility networks can accelerate the spread of infectious diseases by increasing the frequency of close human interactions, particularly in high-rise and transit-dense environments. On the other hand, improved accessibility can strengthen resilience by facilitating faster delivery of essential services, such as food distribution in informal settlements, access to emergency healthcare, and equitable provision of welfare facilities. These dual effects underscore the necessity of incorporating the vertical dimension into 15-minute city planning and implementation worldwide, not only to balance efficiency with public health considerations, but also to adapt accessibility strategies to the diverse socio-economic and spatial realities of different urban contexts.

In addition, this study adopted a fixed walking speed to estimate travel durations, without accounting for speed variations in natural 3D environments. As noted in previous research [82], urban expansion often occurs along sloped terrain, particularly in cities characterized by upslope and downslope conditions, which can be significant in some cities (e.g., San Francisco and Hong Kong) [83] . In such contexts, walking speed may vary significantly due to changes in elevation, slope gradient, and physical exertion [43]. These variations influence not only individual preference for facilities but also route selection and mode choice, which in turn affect the actual proximity to urban services. Incorporating slope-adjusted walking speeds into future models would provide a more realistic estimation of vertical 15-minute city in hilly urban contexts [84]. Meanwhile, the vertical time cost is different for age groups [85]. For example, children and older people should take more time in climbing stairs. These variations have important implications for the inclusiveness of 15-minute city. Accounting for age-specific mobility constraints would allow planners and researchers to evaluate accessibility more equitably and support the development of truly inclusive vertical urban environment. In real-world scenarios, variations in travel time, especially delays caused by elevator waiting during peak hours, also can further diminish accessibility. Future studies should therefore incorporate dynamic travel factors to achieve more refined analyses.

6. Conclusion

We propose a novel conceptual extension and methodological framework for evaluating 3D 15-minute city accessibility at the floor level, which improves analytical resolution and incorporates the vertical dimension into traditional proximity assessments. This study presents an enhanced framework for evaluating 15-minute city accessibility by considering the vertical dimension, regarding high-density urban environments more truthfully. By integrating multi-source urban data, including POIs, AOIs, and land use parcels, we inferred floor-level functional compositions and constructed 3D proximity indices that account for both horizontal network-based travel and vertical movement within buildings. Through this approach, we addressed key challenges in traditional 2D evaluations, such as the neglect of vertical accessibility and the oversimplification of facility distribution in mixed-use buildings.

Our results reveal significant spatial disparities in 15-minute accessibility across different floors and urban zones. Vertical variations in travel time, especially in high-rise settings, can lead to overestimation of accessibility when using conventional 2D metrics. Additionally, we find that 3D spatial access equality is influenced by distance to the urban core ('U-shaped' structure) and have a relationship with GDP level. These findings underscore the need to rethink 3D 15-minute proximity planning in high-density cities, moving beyond planar metrics to consider the vertical complexity of the built environment. Although 15 minute is a fixed threshold, the proposed 3D proximity framework provides a realistic and deep understanding of urban service reachability and offers methodological support for promoting spatial equity in future 15-minute or X-minute city implementations for vertical urban environment.

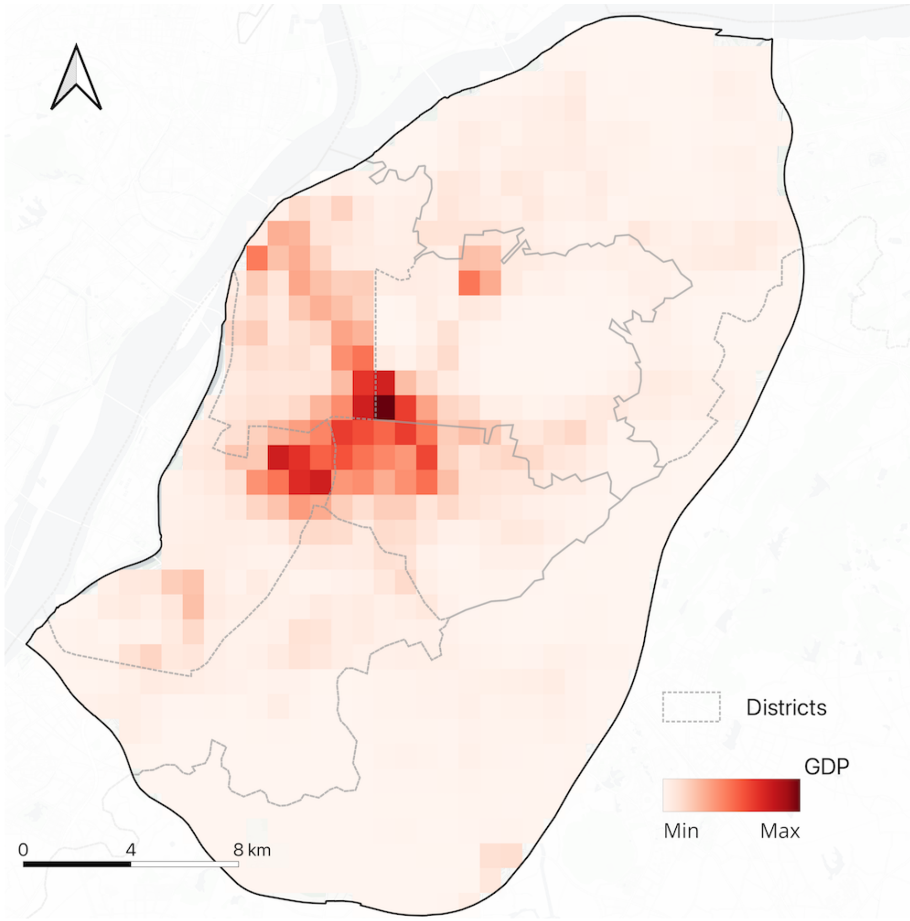

Figure C.15: Spatial map of gridded GDP in the study area

Appendices

Appendix A. The taxonomy and definition of floor facility

Appendix B. Algorithm of extracting 3D facilities

Appendix C. Spatial map of gridded GDP in the study area

Table A.3: The taxonomy and definition of floor facility

Types	**Definition**
Residential	Floors used for housing purposes, including single-family homes, apartment complexes, dormitories, and other living accommodations.
Company	Floors primarily used for work-related activities, including office spaces, industrial manufacturing areas, and development facilities, and other business-related workplaces.
Commerce	Floors designated for commercial activities, such as retail stores, shopping centers, restaurants, cafes, and other service-oriented businesses.
Public Service	Floors occupied by government agencies and public service institutions, including administrative offices, community centers, public safety facilities, and other service infrastructures.
Education	Floors used for educational and research purposes, including schools, universities, research institutes, and related support facilities such as dormitories, canteens, and laboratories.
Medical	Floors designated for healthcare services, including hospitals, clinics, outpatient centers, and other medical service facilities.
Recreation	Floors and land areas used for recreational, cultural, and sports-related activities, such as gyms, fitness centers, libraries, museums, theaters, and exhibition halls.

Algorithm 1: `ExtractFloorLevel(POI, BuildingFootprints)`

```
Input: POI data with address strings, Building footprint polygons
Output: Floor level assigned to each POI, linked to 3D buildings
Function ResolveSpatialMisalignment(POIs, Buildings):
    foreach POI ∈ POIs do
        if POI not intersecting any building then
            Assign POI to nearest building using Voronoi tessellation

Function StandardizeAddressText(address):
    Remove whitespace, dashes, braces and punctuation
    Convert Chinese numerals to Arabic numerals;
    return standardized_address

Function ExtractFloorFromText(standardized_address):
    Tokenize using PKUSEG (mixed mode) ;    /* Segment address into
     meaningful units */
    Search for floor-related tokens and extract adjacent digits;
    if no floor tokens found then
        return floor = 1 ;                   /* Default floor level */
    if token has letter 'B' then
        return Exclude POI (basement)
    if 1–2 digit number then
        return floor = number
    if 3-digit number then
        return floor = first digit ;   /* Use hundreds digit as floor */
    if 4-digit number then
        if first two digits in building's floor range then
            return floor = first two digits ;        /* Validated against
             building floor */
        else
            return floor = second digit ;  /* Fallback to safer guess */

Function AssignFloorLevel(POIs, Buildings):
    ResolveSpatialMisalignment(POIs, Buildings);
    foreach POI do
        standardized_address ← StandardizeAddressText(POI.address);
        floor ← ExtractFloorFromText(standardized_address);
        Link floor to associated 3D building model

Main: AssignFloorLevel(POIs, BuildingFootprints);
```

Table D.4: Performance of Each Block

Block	Accuracy	Precision	F1
Xinjiekou Block	0.902	0.887	0.888
Xuzhuang Block	0.851	0.792	0.737
Xishanqiao Block	0.921	0.834	0.817
Dongshan Block	0.970	0.806	0.814

Appendix D. Performance evaluation of floor-level function

To evaluate the performance of floor-level function identification, four representative sample areas in Nanjing were selected, each characterized by distinct building morphology and functional composition: Xinjiekou Block, Xuzhuang Block, Xishanqiao Block, and Dongshan Block, as shown in Figure D.16.

$$\text{Accuracy} = \frac{\sum_{i=1}^{K} TP_i}{N} = \frac{\text{trace}(\mathbf{CM})}{\sum_{i=1}^{K} \sum_{j=1}^{K} CM_{ij}} \tag{D.1}$$

where TP_i denotes the true positives of class i, N is the total number of samples, and $\mathbf{CM}$ is the confusion matrix. Accuracy measures the overall correctness of the classification.

$$\text{Precision} = \frac{1}{K} \sum_{i=1}^{K} \frac{TP_i}{TP_i + FP_i} \tag{D.2}$$

where FP_i is the false positives of class i. Precision measures how many of the samples predicted as class i are actually correct. The macro average gives equal weight to each class, regardless of its size.

$$F1_i = \frac{2 \cdot \text{Precision}_i \cdot \text{Recall}_i}{\text{Precision}_i + \text{Recall}_i} \tag{D.3}$$

$$\text{F1} = \frac{1}{K} \sum_{i=1}^{K} F1_i \tag{D.4}$$

where $Recall_i = \frac{TP_i}{TP_i+FN_i}$ and FN_i is the false negatives of class i. The F1 score is the harmonic mean of Precision and Recall, balancing correctness and completeness. The macro F1 averages $F1_i$ across classes to evaluate multi-class performance.

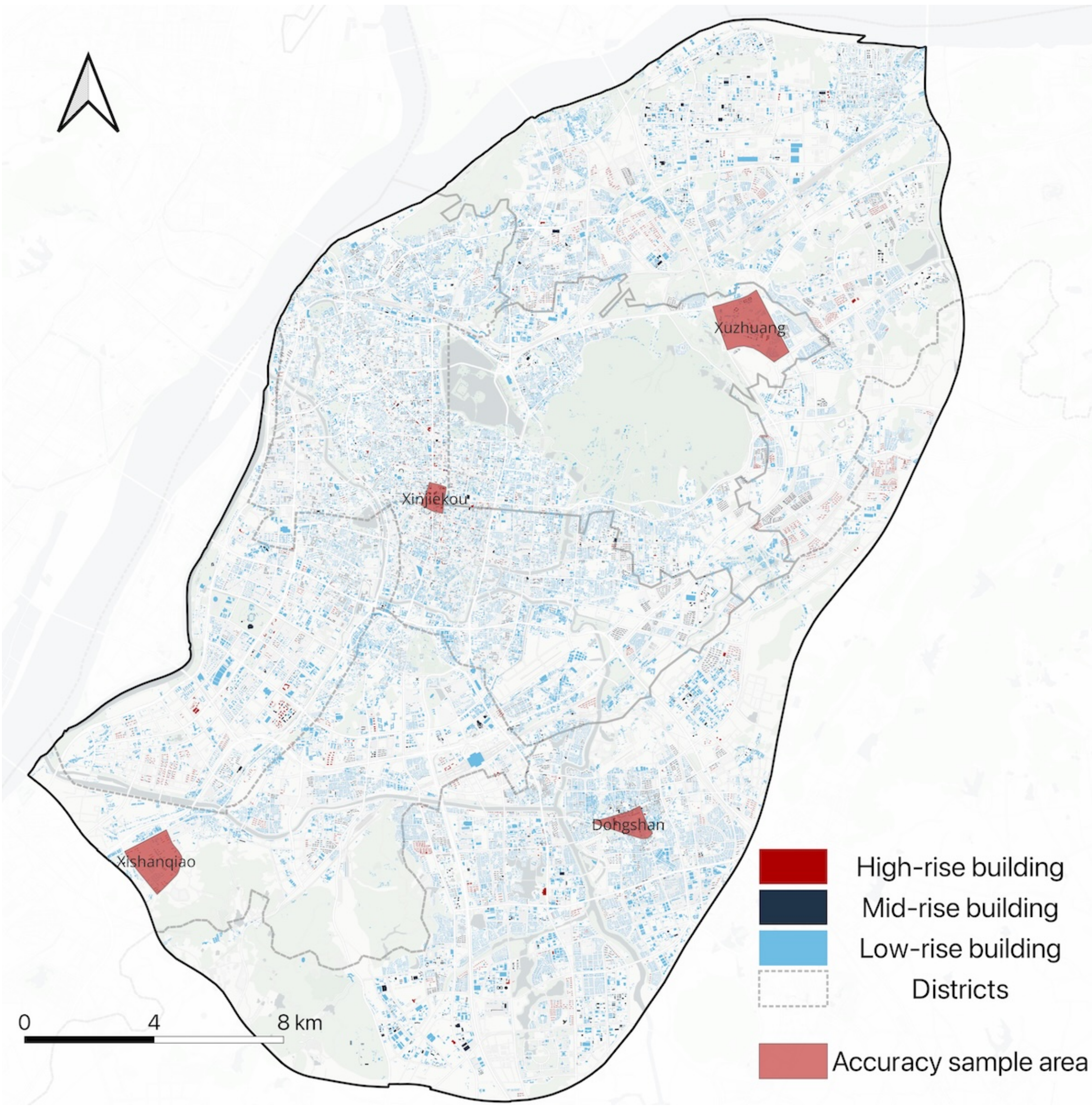

Figure D.16: Four accuracy sampling areas in Nanjing

Figure D.17: Confusion matrix of classification accuracy in the study area.

Declaration of Generative AI and AI-assisted technologies in the writing process

During the preparation of this work, the authors used ChatGPT 4o to improve the readability and language of the manuscript. After using this tool, the authors reviewed and edited the content as needed and take full responsibility for the content of the published article.

References

[1] M. Batty, P. Longley, Fractal cities: a geometry of form and function, Academic press, 1994.

[2] J. Jacobs, The Death and Life of Great American Cities, Random House, New York City, 1961.

[3] Y. Zhou, X. Li, W. Chen, L. Meng, Q. Wu, P. Gong, K. C. Seto, Satellite mapping of urban built-up heights reveals extreme infrastructure gaps and inequalities in the Global South, Proceedings of the National Academy of Sciences 119 (46) (2022) e2214813119. doi:10.1073/pnas.2214813119.

[4] L. Corbusier, Towards a new architecture, Courier Corporation, 2013.

[5] N. Mualam, E. Salinger, D. Max, Increasing the urban mix through vertical allocations: Public floorspace in mixed use development, Cities 87 (2019) 131–141. doi:10.1016/j.cities.2018.12.027.

[6] Z. Chen, L. Tang, X. Guo, G. Zheng, A self-supervised detection method for mixed urban functions based on trajectory temporal image, Computers, Environment and Urban Systems 110 (2024) 102113. doi:10.1016/j.compenvurbsys.2024.102113.

[7] D. Mitchell, S. Claris, D. Edge, Human-centered mobility: A new approach to designing and improving our urban transport infrastructure, Engineering 2 (1) (2016) 33–36. doi:10.1016/J.ENG.2016.01.030.

[8] Y. Yue, Y. Zhuang, A. G. Yeh, J.-Y. Xie, C.-L. Ma, Q.-Q. Li, Measurements of poi-based mixed use and their relationships with neighbourhood vibrancy, International Journal of Geographical Information Science 31 (4) (2017) 658–675. doi:10.1080/13658816.2016.1220561.

[9] L. Yin, Street level urban design qualities for walkability: Combining 2d and 3d gis measures, Computers, Environment and Urban Systems 64 (2017) 288–296. doi:10.1016/j.compenvurbsys.2017.04.001.

[10] P. Liu, T. Zhao, J. Luo, B. Lei, M. Frei, C. Miller, F. Biljecki, Towards human-centric digital twins: Leveraging computer vision and graph models to predict outdoor comfort, Sustainable Cities and Society 93 (2023) 104480. doi:10.1016/j.scs.2023.104480.

[11] E. Zhang, J. Hou, Y. Long, The form of China's urban commercial expansion in the digital era, Nature Cities (2025) 1–11doi:10.1038/s44284-025-00254-6.

[12] E. Elldér, Exploring socio-economic inequalities in access to the 15-minute city across 200 Swedish built-up areas, Journal of Transport Geography 122 (2025) 104060. doi:10.1016/j.jtrangeo.2024.104060.

[13] C. Moreno, Z. Allam, D. Chabaud, C. Gall, F. Pratlong, Introducing the "15-Minute City": Sustainability, Resilience and Place Identity in Future Post-Pandemic Cities, Smart Cities 4 (1) (2021) 93–111. doi:10.3390/smartcities4010006.

[14] A. R. Khavarian-Garmsir, A. Sharifi, A. Sadeghi, The 15-minute city: Urban planning and design efforts toward creating sustainable neighborhoods, Cities 132 (2023) 104101. doi:10.1016/j.cities.2022.104101.

[15] J. F. Teixeira, C. Silva, S. Seisenberger, B. Büttner, B. McCormick, E. Papa, M. Cao, Classifying 15-minute Cities: A review of worldwide practices, Transportation Research Part A: Policy and Practice 189 (2024) 104234. doi:10.1016/j.tra.2024.104234.

[16] Z. Allam, M. Nieuwenhuijsen, D. Chabaud, C. Moreno, The 15-minute city offers a new framework for sustainability, liveability, and health, The Lancet Planetary Health 6 (3) (2022) e181–e183. doi:10.1016/S2542-5196(22)00014-6.

[17] E. Burton, The Compact City: Just or Just Compact? A Preliminary Analysis, Urban Studies 37 (11) (2000) 1969–2006. doi:10.1080/00420980050162184.

[18] M. Neuman, The compact city fallacy, Journal of planning education and research 25 (1) (2005) 11–26. doi:10.1177/0739456X04270466.

[19] M. Southworth, Designing the walkable city, Journal of urban planning and development 131 (4) (2005) 246–257. doi:10.1061/(ASCE)0733-9488(2005)131:4(246).

[20] O. Marquet, C. Miralles-Guasch, The walkable city and the importance of the proximity environments for barcelona's everyday mobility, Cities 42 (2015) 258–266. doi:10.1016/j.cities.2014.10.012.

[21] R. J. Grant, H. Li, A. C. Oner, Legacy of arts and chrono-urbanism in Wynwood, Miami, Cities 159 (2025) 105787. doi:10.1016/j.cities.2025.105787.

[22] E. Talen, J. Koschinsky, et al., The walkable neighborhood: A literature review, International journal of sustainable land use and urban planning 1 (1) (2013) 42–63.

[23] M. Weng, N. Ding, J. Li, X. Jin, H. Xiao, Z. He, S. Su, The 15-minute walkable neighborhoods: Measurement, social inequalities and implications for building healthy communities in urban China, Journal of Transport & Health 13 (2019) 259–273. doi:10.1016/j.jth.2019.05.005.

[24] M. Batty, Accessibility: in search of a unified theory (2009). doi:10.1068/b3602ed.

[25] M. Khatibi, K. A. M. Khaidzir, S. S. Syed Mahdzar, A. Sharifi, Revisiting the neighborhood definition in view of the 15-minute neighborhood and sustainable neighborhood concepts, Cities 162 (2025) 105986. doi:10.1016/j.cities.2025.105986.

[26] B. Sepehri, A. Sharifi, X-minute cities as a growing notion of sustainable urbanism: A literature review, Cities 161 (2025) 105902. doi:10.1016/j.cities.2025.105902.

[27] L. A. Guzman, D. Oviedo, V. A. Cantillo-Garcia, Is proximity enough? A critical analysis of a 15-minute city considering individual perceptions, Cities 148 (2024) 104882. doi:10.1016/j.cities.2024.104882.

[28] S. Zhang, F. Zhen, Y. Kong, T. Lobsang, S. Zou, Towards a 15-minute city: A network-based evaluation framework, Environment and Planning B: Urban Analytics and City Science 50 (2) (2023) 500–514. doi:10.1177/23998083221118570.

[29] J.-C. Thill, T. H. D. Dao, Y. Zhou, Traveling in the three-dimensional city: applications in route planning, accessibility assessment, location analysis and beyond, Journal of Transport Geography 19 (3) (2011) 405–421. doi:10.1016/j.jtrangeo.2010.11.007.

[30] A. Bassolas, H. Barbosa-Filho, B. Dickinson, X. Dotiwalla, P. Eastham, R. Gallotti, G. Ghoshal, B. Gipson, S. A. Hazarie, H. Kautz, et al., Hierarchical organization of urban mobility and its connection with city livability, Nature communications 10 (1) (2019) 4817. doi:10.1038/s41467-019-12809-y.

[31] Z. Allam, A. R. Khavarian-Garmsir, U. Lassaube, D. Chabaud, C. Moreno, Mapping the Implementation Practices of the 15-Minute City, Smart Cities 7 (4) (2024) 2094–2109. doi:10.3390/smartcities4010006.

[32] J. Burke, R. Gras Alomà, F. Yu, J. Kruguer, Geospatial analysis framework for evaluating urban design typologies in relation with the 15-minute city standards, Journal of Business Research 151 (2022) 651–667. doi:10.1016/j.jbusres.2022.06.024.

[33] A. Bartzokas-Tsiompras, , E. Bakogiannis, Quantifying and visualizing the 15-Minute walkable city concept across Europe: a multicriteria approach, Journal of Maps 19 (1) (2023) 2141143. doi:10.1080/17445647.2022.2141143.

[34] D. Vale, A. S. Lopes, Accessibility inequality across Europe: a comparison of 15-minute pedestrian accessibility in cities with 100,000 or more inhabitants, npj Urban Sustainability 3 (1) (2023) 1–13. doi:10.1038/s42949-023-00133-w.

[35] C. Ferrer-Ortiz, O. Marquet, L. Mojica, G. Vich, Barcelona under the 15-Minute City Lens: Mapping the Accessibility and Proximity Potential Based on Pedestrian Travel Times, Smart Cities 5 (1) (2022) 146–161. doi:10.3390/smartcities5010010.

[36] E. Graells-Garrido, F. Serra-Burriel, F. Rowe, F. M. Cucchietti, P. Reyes, A city of cities: Measuring how 15-minutes urban accessibility shapes human mobility in Barcelona, PLOS ONE 16 (5) (2021) e0250080. doi:10.1371/journal.pone.0250080.

[37] T. Jin, K. Wang, Y. Xin, J. Shi, Y. Hong, F. Witlox, Is a 15-Minute City Within Reach? Measuring Multimodal Accessibility and Carbon Footprint in 12 Major American Cities, Land Use Policy 142 (2024) 107180. doi:10.1016/j.landusepol.2024.107180.

[38] E. Papadopoulos, A. Sdoukopoulos, I. Politis, Measuring compliance with the 15-minute city concept: State-of-the-art, major components and further requirements, Sustainable Cities and Society 99 (2023) 104875. doi:10.1016/j.scs.2023.104875.

[39] K. Mouratidis, Time to challenge the 15-minute city: Seven pitfalls for sustainability, equity, livability, and spatial analysis, Cities 153 (2024) 105274. doi:10.1016/j.cities.2024.105274.

[40] E. Willberg, C. Fink, T. Toivonen, The 15-minute city for all?–measuring individual and temporal variations in walking accessibility, Journal of Transport Geography 106 (2023) 103521. doi:10.1016/j.jtrangeo.2022.103521.

[41] M. Weng, N. Ding, J. Li, X. Jin, H. Xiao, Z. He, S. Su, The 15-minute walkable neighborhoods: Measurement, social inequalities and implications for building healthy communities in urban china, Journal of Transport & Health 13 (2019) 259–273. doi:10.1016/j.jth.2019.05.005.

[42] A. Gorrini, D. Presicce, F. Messa, R. Choubassi, Walkability for children in bologna: Beyond the 15-minute city framework, Journal of Urban Mobility 3 (2023) 100052. doi:10.1016/j.urbmob.2023.100052.

[43] D. Rhoads, A. Solé-Ribalta, J. Borge-Holthoefer, The inclusive 15-minute city: Walkability analysis with sidewalk networks, Computers, Environment and Urban Systems 100 (2023) 101936. doi:10.1016/j.compenvurbsys.2022.101936.

[44] E. Knap, M. B. Ulak, K. T. Geurs, A. Mulders, S. Van Der Drift, A composite x-minute city cycling accessibility metric and its role in assessing spatial and

socioeconomic inequalities–a case study in utrecht, the netherlands, Journal of Urban Mobility 3 (2023) 100043. doi:10.1016/j.urbmob.2022.100043.

[45] M. Bruno, H. P. Monteiro Melo, B. Campanelli, V. Loreto, A universal framework for inclusive 15-minute cities, Nature Cities 1 (10) (2024) 633–641. doi:10.1038/s44284-024-00119-4.

[46] C. Birkenfeld, R. Victoriano-Habit, M. Alousi-Jones, A. Soliz, A. El-Geneidy, Who is living a local lifestyle? towards a better understanding of the 15-minute-city and 30-minute-city concepts from a behavioural perspective in montréal, canada, Journal of Urban Mobility 3 (2023) 100048. doi:10.1016/j.urbmob.2023.100048.

[47] B. Caselli, M. Carra, S. Rossetti, M. Zazzi, Exploring the 15-minute neighbourhoods. an evaluation based on the walkability performance to public facilities, Transportation research procedia 60 (2022) 346–353. doi:10.1016/j.trpro.2021.12.045.

[48] T. Logan, T. Williams, A. Nisbet, K. Liberman, C. Zuo, S. Guikema, Evaluating urban accessibility: leveraging open-source data and analytics to overcome existing limitations, Environment and Planning B: Urban Analytics and City Science 46 (5) (2019) 897–913. doi:10.1177/2399808317736528.

[49] S. Zhang, W. Wu, Z. Xiao, S. Wu, Q. Zhao, D. Ding, L. Wang, Creating livable cities for healthy ageing: Cognitive health in older adults and their 15-minute walkable neighbourhoods, Cities 137 (2023) 104312. doi:10.1016/j.cities.2023.104312.

[50] X. Liu, Y. Long, Automated identification and characterization of parcels with openstreetmap and points of interest, Environment and Planning B: Planning and Design 43 (2) (2016) 341–360. doi:10.1177/0265813515604767.

[51] T. Wang, Y. Li, I.-T. Chuang, W. Qiao, J. Jiang, L. Beattie, Evaluating the 15-minute city paradigm across urban districts: A mobility-based approach in Hamilton, New Zealand, Cities 151 (2024) 105147. doi:10.1016/j.cities.2024.105147.

[52] L. Song, X. Kong, P. Cheng, Supply-demand matching assessment of the public service facilities in 15-minute community life circle based on residents' behaviors, Cities 144 (2024) 104637. doi:10.1016/j.cities.2023.104637.

[53] C. Fan, X. Jiang, R. Lee, A. Mostafavi, Equality of access and resilience in urban population-facility networks, npj Urban Sustainability 2 (1) (2022) 1–12. doi:10.1038/s42949-022-00051-3.

[54] T. Abbiasov, C. Heine, S. Sabouri, A. Salazar-Miranda, P. Santi, E. Glaeser, C. Ratti, The 15-minute city quantified using human mobility data, Nature Human Behaviour 8 (3) (2024) 445–455. doi:10.1038/s41562-023-01770-y.

[55] G. Touya, V. Antoniou, A.-M. Olteanu-Raimond, M.-D. Van Damme, Assessing crowdsourced poi quality: Combining methods based on reference data, history, and spatial relations, ISPRS International Journal of Geo-Information 6 (3) (2017) 80. doi:10.3390/ijgi6030080.

[56] K. Sun, Y. Hu, Y. Ma, R. Z. Zhou, Y. Zhu, Conflating point of interest (poi) data: A systematic review of matching methods, Computers, Environment and Urban Systems 103 (2023) 101977. doi:10.1016/j.compenvurbsys.2023.101977.

[57] C. Ye, F. Zhang, L. Mu, Y. Gao, Y. Liu, Urban function recognition by integrating social media and street-level imagery, Environment and Planning B: Urban Analytics and City Science 48 (6) (2021) 1430–1444. doi:10.1177/2399808320935467.

[58] A. Lin, X. Sun, H. Wu, W. Luo, D. Wang, D. Zhong, Z. Wang, L. Zhao, J. Zhu, Identifying urban building function by integrating remote sensing imagery and poi data, IEEE Journal of Selected Topics in Applied Earth Observations and Remote Sensing 14 (2021) 8864–8875. doi:10.1109/JSTARS.2021.3107543.

[59] W. Huang, L. Cui, M. Chen, D. Zhang, Y. Yao, Estimating urban functional distributions with semantics preserved poi embedding, International Journal of Geographical Information Science 36 (10) (2022) 1905–1930. doi:10.1080/13658816.2022.2040510.

[60] Y. Zhang, P. Liu, F. Biljecki, Knowledge and topology: A two layer spatially dependent graph neural networks to identify urban functions with time-series street view image, ISPRS Journal of Photogrammetry and Remote Sensing 198 (2023) 153–168. doi:10.1016/j.isprsjprs.2023.03.008.

[61] Y. Guo, J. Tang, H. Liu, X. Yang, M. Deng, Identifying up-to-date urban land-use patterns with visual and semantic features based on multisource geospatial data, Sustainable Cities and Society 101 (2024) 105184. doi:10.1016/j.scs.2024.105184.

[62] D. Choi, M. Kang, J. Yoon, Utility of mixed-use development by reducing aggregated travel time for multiple non-work activities: A case of Seoul, Korea, Cities 109 (2021) 103007. doi:10.1016/j.cities.2020.103007.

[63] B. Vilhelmson, E. Elldér, Realizing proximity in times of deregulation and densification: Evaluating urban change from a welfare regime perspective, Journal of Transport geography 94 (2021) 103098. doi:10.1016/j.jtrangeo.2021.103098.

[64] Z. Li, J. Zheng, Y. Zhang, Study on the layout of 15-minute community-life circle in third-tier cities based on poi: Baoding city of hebei province, Engineering 11 (9) (2019) 592–603. doi:10.4236/eng.2019.119041.

[65] J. Wan, H. Sun, X. Fan, A. Phillips, Y. Zhao, Y. Chen, Z. Wang, H. Xiao, X. Dong, W. Zhu, Refining the 15-minute community living circle: An innovative evaluation method for medical facility allocation in chengdu, Land Use Policy 145 (2024) 107286. doi:10.1016/j.landusepol.2024.107286.

[66] A. Albashir, F. Messa, D. Presicce, A. Pedrazzoli, A. Gorrini, 15min City Score Toolkit – Urban Walkability Analytics, Tech. rep., Zenodo (Nov. 2024). doi:10.5281/zenodo.14231533.
URL https://zenodo.org/records/14231533

[67] P. Gong, B. Chen, X. Li, H. Liu, J. Wang, Y. Bai, J. Chen, X. Chen, L. Fang, S. Feng, Y. Feng, Y. Gong, H. Gu, H. Huang, X. Huang, H. Jiao, Y. Kang, G. Lei, A. Li, X. Li, X. Li, Y. Li, Z. Li, Z. Li, C. Liu, C. Liu, M. Liu, S. Liu, W. Mao, C. Miao, H. Ni, Q. Pan, S. Qi, Z. Ren, Z. Shan, S. Shen, M. Shi, Y. Song, M. Su, H. Ping Suen, B. Sun, F. Sun, J. Sun, L. Sun, W. Sun, T. Tian, X. Tong, Y. Tseng, Y. Tu, H. Wang, L. Wang, X. Wang, Z. Wang, T. Wu, Y. Xie, J. Yang, J. Yang, M. Yuan, W. Yue, H. Zeng, K. Zhang, N. Zhang, T. Zhang, Y. Zhang, F. Zhao, Y. Zheng, Q. Zhou, N. Clinton, Z. Zhu, B. Xu, Mapping essential urban land use categories in China (EULUC-China): preliminary results for 2018, Science Bulletin 65 (3) (2020) 182–187. doi:10.1016/j.scib.2019.12.007.

[68] Y. Cao, X. Huang, A deep learning method for building height estimation using high-resolution multi-view imagery over urban areas: A case study of 42 Chinese cities, Remote Sensing of Environment 264 (2021) 112590. doi:10.1016/j.rse.2021.112590.

[69] Y. Chen, W. Sun, L. Yang, X. Yang, X. Zhou, X. Li, S. Li, G. Tang, Refining urban morphology: An explainable machine learning method for estimating footprint-level building height, Sustainable Cities and Society 112 (2024) 105635. doi:10.1016/j.scs.2024.105635.

[70] B. Chen, B. Xu, P. Gong, Mapping essential urban land use categories (euluc) using geospatial big data: Progress, challenges, and opportunities, Big Earth Data 5 (3) (2021) 410–441. doi:10.1080/20964471.2021.1939243.

[71] S. Xiong, X. Zhang, Y. Lei, G. Tan, H. Wang, S. Du, Time-series china urban land use mapping (2016–2022): An approach for achieving spatial-consistency and semantic-transition rationality in temporal domain, Remote Sensing of Environment 312 (2024) 114344. doi:10.1016/j.rse.2024.114344.

[72] T. Wang, F. Sun, Global gridded gdp data set consistent with the shared socioeconomic pathways, Scientific data 9 (1) (2022) 221. doi:10.1038/s41597-022-01300-x.

[73] D. Luxen, C. Vetter, Real-time routing with openstreetmap data, in: Proceedings of the 19th ACM SIGSPATIAL International Conference on Advances in Geographic Information Systems, GIS '11, ACM, New York, NY, USA, 2011, pp. 513–516.

[74] R. W. Bohannon, A. Williams Andrews, Normal walking speed: a descriptive meta-analysis, Physiotherapy 97 (3) (2011) 182–189. doi:10.1016/j.physio.2010.12.004.

[75] J. Norén, M. Delin, K. Fridolf, Ascending Stair Evacuation: What do We Know?, Transportation Research Procedia 2 (2014) 774–782. doi:10.1016/j.trpro.2014.09.087.

[76] The impact of elevator speed on building efficiency and user experience, https://southernelevator.com/the-impact-of-elevator-speed-on-building-efficiency-and-user-experience/, accessed: 2025-08-14 (2023).

[77] How fast do elevators move?, https://dazenelevator.com/how-fast-do-elevators-move/, accessed: 2025-08-14 (2023).

[78] H. Cheng, D. Shaw, Polycentric development practice in master planning: the case of China, International Planning Studies 23 (2) (2018) 163–179. doi:10.1080/13563475.2017.1361318.

[79] X. Zhou, A. G. O. Yeh, Y. Yue, Spatial variation of self-containment and jobs-housing balance in Shenzhen using cellphone big data, Journal of Transport Geography 68 (2018) 102–108. doi:10.1016/j.jtrangeo.2017.12.006.

[80] Z. Liu, S. Liu, Polycentric development and the role of urban polycentric planning in china's mega cities: An examination of beijing's metropolitan area, Sustainability 10 (5) (2018) 1588. doi:10.3390/su10051588.

[81] Y. Che, X. Li, X. Liu, Y. Wang, W. Liao, X. Zheng, X. Zhang, X. Xu, Q. Shi, J. Zhu, H. Zhang, H. Yuan, Y. Dai, 3D-GloBFP: the first global three-dimensional building footprint dataset, Earth System Science Data 16 (11) (2024) 5357–5374. doi:10.5194/essd-16-5357-2024.

[82] K. Shi, Y. Cui, S. Liu, Y. Wu, Global Urban Land Expansion Tends To Be Slope Climbing: A Remotely Sensed Nighttime Light Approach, Earth's Future 11 (4) (2023) e2022EF003384. doi:10.1029/2022EF003384.

[83] K. Y. Ng, M. J. Widener, C. P. Tribby, K. C. Tang, K. Koh, 3D walking accessibility in practice: exploring the imperfections from data, method, and assumptions of human-space interaction, International Journal of Geographical Information Science 0 (0) (2025) 1–21. doi:10.1080/13658816.2025.2533326.

[84] D. Liu, Z. Kan, J. Wang, M.-P. Kwan, J. Song, J. Wei, Using spatially explicit high-granularity 3D geospatial data for quantifying public transport walking accessibility inequality and vulnerability in the x-minute city, Cities 166 (2025) 106245. doi:10.1016/j.cities.2025.106245.

[85] V. Milias, A. Psyllidis, Measuring spatial age segregation through the lens of co-accessibility to urban activities, Computers, Environment and Urban Systems 95 (2022) 101829. doi:10.1016/j.compenvurbsys.2022.101829.